

Differential Proteomic Analysis of Hepatocellular Carcinomas from *Ppp2r5d* Knockout Mice and Normal (Knockout) Livers

CAROLINE LAMBRECHT¹, GABRIELA BOMFIM FERREIRA², JUDIT DOMÈNECH OMELLA¹,
LOUIS LIBBRECHT³, RITA DE VOS⁴, RITA DERUA¹, CHANTAL MATHIEU²,
LUT OVERBERGH², ETIENNE WAELEKENS¹ and VEERLE JANSSENS^{1,5}

¹Laboratory of Protein Phosphorylation and Proteomics, Department Cellular and Molecular Medicine, University of Leuven (KU Leuven), Leuven, Belgium;

²Clinical and Experimental Endocrinology, Department Clinical and Experimental Medicine, University of Leuven (KU Leuven), Leuven, Belgium;

³Department of Pathology, Université Catholique de Louvain (UCL), Brussels, Belgium;

⁴Translational Cell and Tissue Research, Department Imaging and Pathology, University of Leuven (KU Leuven), Leuven, Belgium;

⁵LKI, KU Leuven Cancer Institute, Leuven, Belgium

Abstract. *Background:* Hepatocellular carcinoma (HCC) is the major type of primary liver cancer. Mice lacking the tumor-suppressive protein phosphatase 2A subunit B56δ (*Ppp2r5d*) spontaneously develop HCC, correlating with increased *c-MYC* oncogenicity. *Materials and Methods:* We used two-dimensional difference gel electrophoresis-coupled matrix-assisted laser desorption/ionization time-of-flight mass spectrometry to identify differential proteomes of livers from wild-type, non-cancerous and HCC-affected B56δ knockout mice. *Results:* A total of 23 proteins were differentially expressed/regulated in liver between wild-type and non-cancerous knockout mice, and 119 between non-cancerous and HCC knockout mice ('cancer proteins'). Overlap with our reported differential transcriptome data was poor. Overall, 56% of cancer proteins were reported before in HCC proteomics studies; 44% were novel. Gene Ontology analysis revealed cancer proteins mainly associated with liver metabolism (18%) and mitochondria (15%). Ingenuity Pathway Analysis identified 'cancer' and

'gastrointestinal disease' as top hits. *Conclusion:* We identified several proteins for further exploration as novel potential HCC biomarkers, and independently underscored the relevance of *Ppp2r5d* knockout mice as a valuable hepatocarcinogenesis model.

Hepatocellular carcinoma (HCC) is the most common primary liver cancer, and the second leading cause of cancer-related death worldwide (1). Most patients with HCC are diagnosed at an advanced stage due to asymptomatic features during neoplastic progression, and hence their prognosis is grim. Curative therapies, including orthotopic liver transplantation, surgical resection and local destruction, can only be offered to early diagnosed patients, and is complicated by high recurrence rates. Advanced or non-resectable HCC is associated with a poor prognosis due to broad resistance to chemotherapeutic agents (2-5). Several risk factors for HCC development have been established, including viral hepatitis B and C infection, aflatoxin B1 exposure, excessive alcohol abuse and nonalcoholic fatty liver disease, all giving rise, to some extent, to (chronic) liver inflammation, cirrhosis or liver injury. Only in about 15% of cases does HCC arise in a context of normal liver (6).

In general, the molecular mechanisms resulting in HCC initiation and progression remain incompletely understood (7). In recent years, comparative genomic profiling, gene expression and exome mutational analysis studies in human HCC samples have enabled HCCs to be classified into two different molecular subgroups, termed 'proliferation' and 'nonproliferation' [reviewed in (8, 9)]. Tumors from the first class are highly heterogeneous and are associated with poor prognosis. They show increased protein kinase B (AKT)/mammalian target of rapamycin (mTOR), hepatocyte

This article is freely accessible online.

Correspondence to: Professor V. Janssens, Gasthuisberg O&N1, Herestraat 49, PO-box 901, B-3000 Leuven, Belgium. Tel: +32 16330684, e-mail: Veerle.janssens@kuleuven.be or Professor E. Waelkens, Gasthuisberg O&N1, Herestraat 49, PO-box 901, B-3000 Leuven, Belgium. Tel: +32 16330645, e-mail: Etienne.waelkens@kuleuven.be

Key Words: HCC, PP2A, tumor suppressor, *Ppp2r5d*, B56δ subunit, 2D-DIGE, biomarker, mouse model, hepatocarcinogenesis, fibrinogen, liver, proteomics.

growth factor receptor (MET), transforming growth factor β (TGF β), insulin-like growth factor (IGF), rat sarcoma virus oncogene (RAS)/mitogen-activated protein kinase (MAPK) or NOTCH signaling, high-level amplifications of chromosomes 11q13 [fibroblast growth factor 19 gene (*FGF19*)/cyclin D1 gene (*CCND1*)] or 6p21 [vascular endothelial growth factor A gene (*VEGFA*)], and frequent aberrations in chromosomes 1 or 8 [myelocytomatosis oncogene (*MYC*)]. Tumors from the second class are less aggressive, better differentiated and are associated with a better outcome. They feature activated WNT signaling (mostly *via* β 1-catenin gene (*CTNNB1*) mutations) or chromosome 7 gain [epidermal growth factor receptor gene (*EGFR*)]. The most prevalent mutations in HCC pathogenesis include those in the telomerase reverse transcriptase gene (*TERT*) promoter, tumor protein p53 gene (*TP53*), *CTNNB1*, axin1 gene (*AXIN1*), and AT-rich interaction domain 1A and 2 genes (*ARID1A* and *ARID2*) (10, 11). Up to 10 different mutational signatures associated with HCC have been identified in various studies [reviewed in (8)]. Additional proteomics studies have further contributed to HCC classification and biomarker discovery (12-33). Disappointingly, however, these insights have not yet resulted in improved, molecular-targeted therapies.

To help unraveling the molecular mechanisms underlying hepatocarcinogenesis in different pre-clinical settings *in vivo*, rodent HCC models remain valuable tools. This is especially true for models in which the human pathology is well mimicked, and considering that available human HCC tissues can be limiting. In addition to chemically or virally induced liver cancer models, several genetically engineered transgenic, knockout (KO) or knockin (KI) mouse models of HCC have been described, each featuring its own specific tumor initiation/progression, tumor microenvironment and mechanistic characteristics [reviewed in (34, 35)]. These models have significantly contributed to identifying molecular signatures relevant to HCC *via* cross-species comparative and integrative analyses with human data. Moreover, they have facilitated the discovery of potential biomarkers for diagnostic or prognostic purposes.

Recently, we described significantly increased spontaneous HCC development, arising within a largely normal liver context (36), in *Ppp2r5d* KO mice. These mice lack expression of the regulatory B56 δ subunit of protein phosphatase 2A (PP2A) (37), a large family of predominantly tumor-suppressive Ser/Thr protein phosphatases (38, 39) regulating cell signaling processes in many organs and tissues (40). Tumor-suppressive PP2A holoenzymes negatively control a large variety of oncogenic pathways, relevant for HCC, including phosphatidylinositol 3-kinase (PI3K)/AKT, mTOR/p70 ribosomal S6 Kinase (p70 S6K), MAP-extracellular signal-regulated kinase (MEK)/extracellular signal-regulated kinase (ERK) and WNT signaling (41).

Mechanistically, we identified lack of PP2A-B56 δ -driven glycogen synthase kinase-3 β (GSK-3 β) dephosphorylation on Ser9 (resulting in constitutive GSK-3 β inactivation) as the likely tumor-predisposing factor, which affected the GSK-3 β substrate c-MYC in all HCC-bearing livers. Indeed, in the presence of a serendipitous oncogenic alteration affecting c-MYC Ser62 phosphorylation, lack of c-MYC Thr-58 phosphorylation by GSK-3 β resulted in c-MYC stabilization and Ser62 hyperphosphorylation in all tumors (36). c-MYC is a well-established oncogenic driver in liver (42, 43), whose activation is essential for malignant conversion of dysplastic nodules into early HCC (44). Conversely, PP2A-B56 δ appears to act as a tumor suppressor in liver, keeping oncogenic activation of c-MYC in check (36).

HCCs from several c-MYC transgenic mouse models show interesting molecular overlaps with human HCCs of both the better and the poorer survival groups (45). In the present study, we subjected B56 δ KO HCC samples, paired non-cancerous B56 δ KO liver tissue, and wild-type (WT) livers to an unbiased quantitative proteomics approach using two-dimensional difference gel electrophoresis (2D-DIGE). With this approach, we aimed to provide further insights into the mechanisms of hepatocarcinogenesis in *Ppp2r5d* KO mice, as well as into the suitability of this model to mimic human HCC.

Materials and Methods

Sampling of biological material. All protocols involving mice were in compliance with the KU Leuven University Animal Care and Usage Committee (ECD projects P034-2008 and P168-2013). The genetic background of the WT and *Ppp2r5d* KO mice was mixed (C57BL/6;129 - 87.5%;12.5%) (F3) (36). All sampled mice were male and between 18 and 24 months old. Mice were anaesthetized with an intraperitoneal injection of pentobarbital (Nembutal) and transcardially perfused with ice-cold saline (NaCl 0.9% Baxter). Livers were entirely removed, or in the case of a macroscopically visible liver lesion, both the lesion and a part of the normal surrounding liver were kept separately. For each tissue, one part was fixed in 4% paraformaldehyde at 4°C overnight, washed the next day and stored in 70% ethanol until paraffin embedding; another part was snap-frozen in liquid nitrogen and kept at -80°C until further use.

Histopathology. Hematoxylin/eosin-stained sections (4 μ m) of paraffin-embedded liver were examined by a liver pathologist for the presence of pathological lesions. For the *Ppp2r5d* KO samples, the 'healthy', non-tumor state, as well as the HCC state, were additionally confirmed on a cryosection of the snap-frozen material that was eventually lysed for 2D-DIGE use.

Electron microscopy. Small samples from the snap-frozen tissues were thawed and fixed in 2.5% glutaraldehyde (in 0.1 M phosphate buffer, pH 7.2) at 4°C overnight. After 1 h post-fixation in 2% osmium tetroxide (in 0.1 M phosphate buffer, pH 7.2) at 4°C, the samples were dehydrated in a graded series of ethanol, and embedded in epoxy resin. Ultrathin sections of 50-60 nm were cut,

stained with uranyl acetate and lead citrate, and examined at 50 kV using a Zeiss EM 900 electron microscope (Carl Zeiss AG, Oberkochen, Germany).

Protein extraction and 2D-DIGE. Frozen liver tissues were weighed, homogenized and sonicated on ice in lysis buffer [7 M urea, 2 M thiourea, 40 mM Tris, 1% dithiothreitol (DTT), 4% CHAPS] containing protease and phosphatase inhibitor cocktail (Roche). Samples were centrifuged for 15 min at 20,000 × *g* at 4°C. The supernatant was collected and desalted by dialysis (PlusOne Mini Dialysis kit; GE Healthcare, Chicago, IL, USA), and the protein concentration was determined with the Bradford method. Fifty micrograms of protein was labeled with 200 pmol of amine reactive cyanine dyes Cy3 (samples of condition 1) or Cy5 (samples of condition 2), whereas 50 µg of an internal standard was labeled with 200 pmol of Cy2 (GE Healthcare). The internal standard consisted of a pool of equal amounts of all 12 samples. A total of 12 gels were run, each with three samples (condition 1 sample, condition 2 sample and internal standard). Thus, a WT liver sample (n=4) was compared with a healthy KO liver sample (n=4) (4 gels), as well as with a KO HCC sample (n=4) (4 gels); and a healthy KO liver sample (n=4) was pairwise compared with a KO HCC sample (n=4) (4 gels). IPG strips were rehydrated overnight in 450 µl rehydration buffer [7 M urea, 2 M thiourea, 4% CHAPS, 0.5% immobilized pH gradient (IPG) buffer with either 1% DTT for IPG strips pH 4-7 or 1.2% DeStreak (GE Healthcare) for IPG strips pH 6-9]. The pooled labelled samples containing sample loading buffer were loaded into individual 24 cm IPG strips using anodic cup loading. Isoelectric focusing (first dimension) was carried out on an Ettan IPGphor II manifold (GE Healthcare). After isoelectric focusing, the IPG strips were equilibrated during two intervals of 15 min each in equilibration buffer (7 M urea, 2 M thiourea, 4% CHAPS, 0.5% IPG buffer, 0.02% bromophenol blue), and either 1% DTT (pH strip 4-7) or 1.2% DeStreak (pH strip 6-9). Equilibrated strips were placed on top of a 12.5% sodium dodecyl sulfate polyacrylamide gel and separated on an Ettan DaltSix System (GE Healthcare). Gels were scanned on a Typhoon 9400 gel imager at 100 µm pixel size (GE Healthcare). Prior to analysis with DeCyder V 7.0 software (GE Healthcare), gel images were cropped using ImageQuant TL (GE Healthcare). Spot detection and matching was performed automatically using the “Batch Processor” module of DeCyder V 7.0 software followed by careful manual rematching of unmatched spots and wrongly matched spots. Proteins in spots were accepted as being differentially expressed when showing a statistically significant (*p*<0.05) increase or decrease when compared to the control in at least 75% of the spot maps (Supplementary Table: available at <https://gbiomed.kuleuven.be/lambrecht-cgp>).

Spot digestion and protein identification by matrix-assisted laser desorption/ionization (MALDI) time-of-flight (TOF)/TOF analysis. A pick list was generated and exported into Spot Picker V1.20 software operating the Ettan Spot Picker (GE Healthcare). Spots were picked in MilliQ water, transferred to 100 µl of fixation solution (50% methanol, 5% acetic acid and 45% MilliQ) and rinsed three times with MilliQ water and three times with acetonitrile (ACN) (Sigma-Aldrich, St. Louis, MO, USA). The gel pieces were hydrated in a 100 mM NH₄HCO₃ solution for 10 min followed by a dehydration step in 100% ACN for 10 min with vigorous vortexing. This step was repeated twice prior to dehydrating the gel pieces in a SpeedVac (Thermo Fisher Scientific, Bremen, Germany). The gel pieces were rehydrated in digestion buffer [50 mM

NH₄HCO₃, 5 mM CaCl₂, 5 ng/µl of sequencing grade modified trypsin (Promega, Madison, WI, USA)] on ice for 45 min, followed by overnight incubation at 37°C. The resulting peptides were extracted out of the gel plugs in four steps: once with 50 mM NH₄HCO₃, twice with 50% ACN/5% formic acid, and once with 95% ACN/5% formic acid (30 min each). Supernatants were dried in a SpeedVac. Upon concentrating and desalting the tryptic fragments using ZipTip C-18 (Millipore, Milford, MA, USA), the samples were mixed in a 1:1 ratio with α-cyano-4-hydroxycinnamic acid matrix (saturated solution in 50% ACN/2.5% trifluoroacetic acid in HPLC water), spotted onto the MALDI target plate, and allowed to air dry. MS/MS analyses were performed on a 4800 MALDI TOF/TOF (Applied Biosystems, Waltham, MA, USA). Measurements were taken in the positive ion mode between 900 and 3000 *m/z*. Sequences were automatically acquired by scanning first in MS mode and selecting the 15 most intense ions for MS/MS using an exclusion list of peaks arising from tryptic autodigestion. Air was used as the collision gas, whereas the collision energy was adapted automatically. Data interpretation was carried out using the GPS Explorer software and database searching was carried out using MASCOT. MS/MS searches were conducted with the following settings: Swiss-Prot-TrEMBL as databases, taxonomy *Mus musculus*, MS/MS tolerance for precursor ions was set on 0.2 Da and for fragment ions 0.4 Da, methionine oxidation as variable modification, and carbamidomethylation of cysteine as fixed modification. Only peptides with MASCOT scores above the identity threshold and probability-based MOWSE scores greater than the given cut-off value for MS/MS fragmentation data were retained and taken as significant (*p*<0.05). Using these parameters, 118 picked spots could be linked to at least one reliable protein identification (Supplementary Table: available at <https://gbiomed.kuleuven.be/lambrecht-cgp>). For proteins confirmed to be present within different spots, either in horizontal spot ‘trains’ or dispersed over the whole gel map (32 in total), an average relative abundance value was calculated, keeping up-regulated values separate from down-regulated ones (when applicable). These average values were used for eventual representation in Table I.

Immunoblotting. Protein lysates were resolved on 4-12% 2,2-bis(hydroxymethyl)-2,2',2''-nitrioltriethanol, 2-bis(2-hydroxyethyl) amino-2-(hydroxymethyl)-1,3-propanediol, bis(2-hydroxyethyl)amino-tris(hydroxymethyl)methane (BIS-TRIS) gels (BioRad, Hercules, CA, USA) and transferred to polyvinylidene difluoride membranes (GE Healthcare) by wet blotting. The membranes were blocked in 5% milk in tris(hydroxymethyl)aminomethane-buffered saline (TBS)/Tween buffer (0.1% Tween-20 in TBS) at 4°C overnight. After washing in TBS/Tween, incubation with the primary antibody was performed in TBS/Tween containing 5% bovine serum albumin. The following primary antibodies were used: polyclonal rabbit anti-B56δ (46) (dilution: 1/2,000); monoclonal mouse anti-PP2A A and PP2A C (clones C5.3D10 and F2.6A10, dilution: 1/3,000; kind gifts of Dr. Stephen Dilworth, UK); monoclonal mouse anti-vinculin (dilution: 1/10,000; Sigma-Aldrich), polyclonal rabbit anti-fructose-1,6-bisphosphatase 1 (FBP1) (dilution: 1/1,000; Abcam, Cambridge, UK); mouse monoclonal anti-phosphoglycerate mutase 2 (PGM2) (sc-376718; dilution: 1/500; Santa Cruz Biotechnologies, La Jolla, CA, USA); mouse monoclonal anti-S-adenosylmethionine synthase 1 (METK1) (sc-166452, dilution 1/500; Santa Cruz Biotechnologies); polyclonal rabbit anti-phospho-MEK1/2 S217/S221 (dilution 1/1,000; Cell Signaling Technology, Danvers, MA, USA); polyclonal rabbit anti-phospho-ERK1/2 T202/Y204 (dilution

Table I. Representation of 129 differentially expressed proteins [green: up-regulated, $p < 0.05$; red: down-regulated, $p < 0.05$; grey: not dysregulated, $p > 0.05$; bold: marker proteins confirmed in other proteomics studies of mouse, rat or human hepatocellular carcinoma, including references (last column)].

| Gene name | UniProtKB name | Accession number | Full protein name | Average ratio | | Number of spots | Functional classes GO annotation | Reference |
|------------------|----------------|------------------|--|---------------|-------|-----------------|----------------------------------|---|
| | | | | HCC/KO | KO/WT | | | |
| <i>Ppp2r1A</i> | 2AAA | Q76MZ3 | PP2A 65 kDa regulatory subunit A α or A β | 2.24 | -1.15 | 2 | Cell cycle | Conflict (25) |
| <i>Ccdc15</i> | CCDC15 | Q8C9M2 | Coiled-coiled domain protein15 | 4.92 | -1.55 | 1 | Cell cycle | NEW |
| <i>Ahctf1</i> | ELYS | Q8CJF7 | Protein ELYS | 2.88 | -1.32 | 1 | Cell cycle | NEW |
| <i>Rbbp7</i> | RBBP7 | Q60973 | Histone-binding protein RBBP7 | 2.51 | -1.02 | 1 | Cell cycle | NEW |
| <i>Serpina1b</i> | A1AT2 | P22599 | Alpha-1-antitrypsin 1-2 | 2.68 | -1.64 | 1 | Coagulation | (13, 14, 22, 25-27, 32) |
| <i>Serpinc1</i> | ANT3 | P32261 | Antithrombin-III | 2.06 | -1.14 | 3 | Coagulation | NEW |
| <i>Anxa3</i> | ANXA3 | O35639 | Annexin A3 | 1.9 | 1.28 | 1 | Coagulation | (15) |
| <i>Fgg</i> | FIBG | Q8VCM7 | Fibrinogen gamma chain | 7.28 | -1.1 | 1 | Coagulation | (13) |
| <i>Tcp1</i> | TCPA | P11983 | T-Complex protein 1 subunit alpha | -2.56 | -1.83 | 1 | Coagulation | (15) |
| <i>Cct8</i> | TCPQ | P42932 | T-Complex protein 1 subunit theta | 2.13 | -1.28 | 2 | Coagulation | NEW |
| <i>Anxa11</i> | ANXA11 | P97384 | Annexin A11 | 1.9 | 1.28 | 1 | Cytoskeleton | NEW |
| <i>Anxa4</i> | ANXA4 | P97429 | Annexin A4 | 3.91 | -1.48 | 1 | Cytoskeleton | Conflict (20) |
| <i>Cdh23</i> | CAD23 | Q99PF4 | Cadherin-23 | 1.83 | -1.07 | 1 | Cytoskeleton | NEW |
| <i>Col6a2</i> | CO6A2 | Q02788 | Collagen alpha-2 (VI) chain | -3.7 | 1.71 | 1 | Cytoskeleton | NEW |
| <i>Des</i> | DESM | P31001 | Desmin | 3.51 | -1.19 | 1 | Cytoskeleton | NEW |
| <i>Ezr</i> | EZRI | P26040 | Ezrin | -1.5 | -1.01 | 1 | Cytoskeleton | NEW |
| <i>Krt18</i> | K1C18 | P05784 | Keratin, type I cytoskeletal 18 | 3.69 | -1.28 | 1 | Cytoskeleton | (19, 26, 31) |
| <i>Krt2</i> | K22E | Q3TTY5 | Keratin, type II cytoskeletal 2 epidermal | 3.51 | -1.19 | 1 | Cytoskeleton | (27) |
| <i>Krt77</i> | K2C1B | Q6IFZ6 | Keratin, type II cytoskeletal 1b | 3.51 | -1.19 | 1 | Cytoskeleton | (27) |
| <i>Krt8</i> | K2C8 | P11679 | Keratin type II, cytoskeletal 8 | 4.03 | -1.19 | 5 | Cytoskeleton | (15, 17, 19, 24) |
| <i>Rdx</i> | RADI | P26043 | Radixin | -1.93 | -1.03 | 1 | Cytoskeleton | (19) |
| <i>Tuba1a</i> | TBA1A | P68369 | Tubulin alpha-1A chain | 2.58 | -1.02 | 3 | Cytoskeleton | NEW |
| <i>Tuba1a</i> | TBA1A | P68369 | Tubulin alpha-1A chain | -2.66 | 1.33 | 1 | Cytoskeleton | |
| <i>Tubb2a</i> | TBB2A | Q7TMM9 | Tubulin beta 2A chain | 2.76 | -1.03 | 2 | Cytoskeleton | (25, 33) |
| <i>Tubb2c</i> | TBB2C | AAH05547 | Tubulin beta 2C chain | 2.76 | -1.03 | 2 | Cytoskeleton | (25, 26) |
| <i>Tubb5</i> | TBB5 | P99024 | Tubulin beta-5 chain | 1.94 | -1.06 | 1 | Cytoskeleton | (25) |
| <i>Vim</i> | VIME | P20152 | Vimentin | 2.47 | -1.03 | 2 | Cytoskeleton | (17, 26, 27) |
| <i>Wdr1</i> | WDR1 | O88342 | WD Repeat-containing protein 1 | 1.17 | -1.35 | 2 | Cytoskeleton | |
| <i>Calr</i> | CALR | P14211 | Calreticulin | 2.41 | -1.25 | 1 | ER/protein folding | (31) |
| <i>Dnajc3</i> | DNAJC3 | Q91YW3 | DnaJ homolog subfamily C member 3 | 5.39 | -1.25 | 1 | ER/protein folding | (21) |
| <i>Hsp90b1</i> | ENPL | P08113 | Endoplasmic reticulum chaperone | 3.4 | -1.24 | 1 | ER/protein folding | (21, 27) |
| <i>Erp44</i> | ERP44 | Q9D1Q6 | Endoplasmic reticulum resident protein 44 | -1.17 | -1.41 | 1 | ER/protein folding | |
| <i>Hspa5</i> | GRP78 | P20029 | 78-kDa Glucose-regulated protein | 3.46 | -1.41 | 2 | ER/protein folding | (14, 22, 24, 26, 27, 31) |
| <i>Hspa8</i> | HSP7C | P63017 | Heat-shock cognate 71-kDa protein | 4.08 | -1.08 | 1 | ER/protein folding | (21, 23, 26, 27, 31) |
| <i>P4hb</i> | PDIA1 | P09103 | Protein disulfide-isomerase | 3.25 | -1.63 | 5 | ER/protein folding | (19, 20, 26, 27, 31) |
| <i>Pdia3</i> | PDIA3 | P27773 | Protein disulfide-isomerase A3 | 2.80 | -1.32 | 4 | ER/protein folding | (17, 31) |
| <i>Txndc5</i> | TXND5 | Q91W90 | Thioredoxin domain-containing protein 5 | -1.17 | -1.41 | 1 | ER/protein folding | |
| <i>Eno1</i> | ENOA | P17182 | Alpha-enolase | -2.11 | 1.23 | 2 | Glucose metabolism | (17, 26) |
| <i>Eno3</i> | ENOB | P21550 | Beta-enolase | -1.76 | 1.19 | 1 | Glucose metabolism | NEW |
| <i>Fbp1</i> | FBP1 | Q9QXD6 | Fructose-1,6-bisphosphatase 1 | -1.4 | -1.46 | 2 | Glucose metabolism | (12, 13, 15, 17-20, 22, 26, 27, 31-33) |
| <i>Pgk1</i> | PGK1 | P09411 | Phosphoglycerate kinase 1 | -3.4 | 1.27 | 1 | Glucose metabolism | (26, 31) |
| <i>Pgm2</i> | PGM2 | Q7TSV4 | Phosphoglucomutase-2 | -2.95 | -1.08 | 1 | Glucose metabolism | NEW |
| <i>Tpi1</i> | TPIS | P17751 | Triosephosphate isomerase | -2.05 | -1.12 | 1 | Glucose metabolism | (21) |
| <i>Apoa1</i> | APOA1 | Q00623 | Apolipoprotein A-1 | 15.57 | -0.83 | 5 | Lipids | (22, 25, 31) |
| <i>Cpne1</i> | CPNE1 | Q8C166 | Copine-1 | 1.86 | -1.29 | 1 | Lipids | NEW |
| <i>Aspg</i> | LPP60 | A0JNU3 | 60-kDa Lysophospholipase | 2.5 | -1.42 | 1 | Lipids | (21) |

Table I. Continued

Table I. *Continued*

| Gene name | UniProtKB name | Accession number | Full protein name | Average ratio | | Number of spots | Functional classes GO annotation | Reference |
|----------------|----------------|------------------|---|---------------|-------|-----------------|----------------------------------|-------------------------------------|
| | | | | HCC/KO | KO/WT | | | |
| <i>Got1</i> | AATC | P05201 | Aspartate aminotransferase, cytoplasmic | 1.7 | -1.14 | 1 | Liver metabolism | Conflict (20) |
| <i>Adk</i> | ADK | P55264 | Adenosine kinase | -2.38 | -1.24 | 2 | Liver metabolism | (25) |
| <i>Apmap</i> | APMAP | Q9D7N9 | Adipocyte plasma-membrane associated protein | -3.44 | 1.77 | 1 | Liver metabolism | NEW |
| <i>Ass1</i> | ASSY | P16460 | Argininosuccinate synthase | -3.4 | 1.27 | 1 | Liver metabolism | (17, 20, 26, 28, 31) |
| <i>Bhmt</i> | BHMT1 | O35490 | Betaine homocysteine S-methyltransferase 1 | -3.4 | 1.27 | 1 | Liver metabolism | 13, 14, 18, 20, 21, 26, 29, 30, 33) |
| <i>Cndp2</i> | CNDP2 | Q9D1A2 | Cytosolic non-specific dipeptidase | 2.35 | 1.18 | 1 | Liver metabolism | NEW |
| <i>Dpys</i> | DPYS | Q9EQF5 | Dihydropyrimidinase | -1.73 | -1.1 | 1 | Liver metabolism | NEW |
| <i>Ces7</i> | EST7 | EDL11102 | Carboxylesterase 7 | 2.94 | -1.32 | 2 | Liver metabolism | NEW |
| <i>Aldh1l1</i> | FTHFD | Q8R0Y6 | 10-formyltetrahydrofolate dehydrogenase | -2.98 | 1.13 | 2 | Liver metabolism | (15, 25, 27) |
| <i>Gnmt</i> | GNMT | Q9QXF8 | Glycine N-methyl transferase | -3.62 | 1.09 | 1 | Liver metabolism | (13-15, 22, 25, 26, 31) |
| <i>Gda</i> | GUAD | Q9R111 | Guanine deaminase | -3.09 | 1.9 | 1 | Liver metabolism | NEW |
| <i>Ephx2</i> | HYES | P34914 | Epoxide hydrolase 2 | 2.3 | -1.27 | 1 | Liver metabolism | (31) |
| <i>Mdh1</i> | MDHC | P14152 | Malate dehydrogenase, cytoplasmic | -1.92 | 1.07 | 1 | Liver metabolism | (15, 18, 22, 25) |
| <i>Mat1a</i> | METK1 | Q91X83 | S-Adenosylmethionine synthase isoform type-1 | 7.28 | -1.1 | 1 | Liver metabolism | (12, 31) |
| <i>Mat1a</i> | METK1 | Q91X83 | S-Adenosylmethionine synthase isoform type-1 | -3.09 | 1.9 | 1 | Liver metabolism | (13, 14) |
| <i>P4ha2</i> | P4HA2 | Q60716 | Prolyl 4-hydroxylase subunit alpha 2 | 2.88 | -1.32 | 1 | Liver metabolism | (18) |
| <i>Pbld1</i> | PBLD1 | Q9DCG6 | Phenazine biosynthesis-like containing protein 1 | -2 | 1 | 1 | Liver metabolism | (26) |
| <i>Pah</i> | PH4H | P16331 | Phenylalanine-4-hydroxylase | 3.59 | 1.15 | 1 | Liver metabolism | (15, 19) |
| <i>Pon3</i> | PON3 | Q62087 | Serum paraoxonase/lactonase 3 | 4 | 1.05 | 1 | Liver metabolism | NEW |
| <i>Ctps1</i> | PYRG1 | P70698 | CTP synthase 1 | 2.04 | -1.06 | 1 | Liver metabolism | NEW |
| <i>Ahcy</i> | SAHH | P50247 | Adenosyl homocysteinase | -2.41 | 1.33 | 1 | Liver metabolism | (13, 22, 31) |
| <i>Uap1l1</i> | UAP1L | Q3TW96 | UDP-N-acetylhexosamine pyrophosphorylase-like protein 1 | 4.6 | 1.2 | 1 | Liver metabolism | (15) |
| <i>Acsml</i> | ACSM1 | Q91VA0 | Acyl-coenzyme A synthetase ACSM1, mitochondrial | -1.15 | -1.35 | 1 | Mitochondria | |
| <i>Metap1d</i> | AMP1D | Q9CPW9 | Methionine aminopeptidase 1D, mitochondrial | 1.43 | -1.07 | 1 | Mitochondria | NEW |
| <i>Atp5pd</i> | ATP5H | Q9DCX2 | ATP synthase subunit d, mitochondrial | -1.1 | -1.19 | 1 | Mitochondria | NEW |
| <i>Hspd1</i> | CH60 | P63038 | 60-kDa Heat-shock protein, mitochondrial | 4.6 | 1.2 | 1 | Mitochondria | (23) |
| <i>Cps1</i> | CPS1 | Q8C196 | Carbamoyl-phosphate synthase, mitochondrial | -2.36 | 1.71 | 12 | Mitochondria | (14, 17, 19, 22, 25, 26, 29, 31) |
| <i>Sdha</i> | SDHA | Q8K2B3 | Succinate dehydrogenase flavoprotein subunit, mitochondrial | -1.39 | -1.36 | 3 | Mitochondria | NEW |
| <i>Hspa9</i> | GRP75 | P38647 | Stress-70 protein, mitochondrial | 8.54 | -1.35 | 2 | Mitochondria | (22, 26) |
| <i>Hmgcs2</i> | HMGCS2 | P54869 | Hydroxymethylglutaryl-CoA synthase, mitochondrial | 1.7 | -1.14 | 1 | Mitochondria | (19, 23, 29) |
| <i>Immt</i> | IMMT | Q8CAQ8 | Mitochondrial inner membrane protein | -1.5 | -1.01 | 1 | Mitochondria | NEW |
| <i>Mccc1</i> | MCCA | Q99MR8 | Methylcrotonoyl-CoA carboxylase subunit α, mitochondrial | 5.92 | 1.52 | 1 | Mitochondria | (21) |
| <i>Ndufs2</i> | NDUS2 | Q91WD5 | NADH dehydrogenase iron-sulfur protein 2, mitochondrial | -3.44 | 1.77 | 1 | Mitochondria | NEW |
| <i>Ndufv2</i> | NDUFV2 | Q9D6J6 | NADH dehydrogenase flavoprotein 2, mitochondrial | 35.28 | -1.3 | 1 | Mitochondria | NEW |
| <i>Oat</i> | OAT | P29758 | Ornithine aminotransferase, mitochondrial | 1.52 | -1.19 | 1 | Mitochondria | (15, 19, 25) |

Table I. *Continued*

Table I. Continued

| Gene name | UniProtKB name | Accession number | Full protein name | Average ratio | | Number of spots | Functional classes GO annotation | Reference |
|-----------------|----------------|------------------|---|---------------|-------|-----------------|----------------------------------|--------------------------|
| | | | | HCC/KO | KO/WT | | | |
| <i>Ogdh</i> | ODO1 | Q60597 | 2-oxoglutarate dehydrogenase, mitochondrial | -1.81 | 1.66 | 1 | Mitochondria | |
| <i>Dlst</i> | ODO2 | Q9D2G2 | Dihydrolipoyllysine-residue succinyl-transferase component of 2-oxoglutarate dehydrogenase complex, mitochondrial | 1.59 | -1.17 | 1 | Mitochondria | |
| <i>Otc</i> | OTC | P11725 | Ornithine carbamoyl transferase, mitochondrial | -2.54 | 1.01 | 1 | Mitochondria | (22, 25, 31) |
| <i>Pc</i> | PYC | Q05920 | Pyruvate carboxylase, mitochondrial | -2.33 | 1.18 | 2 | Mitochondria | NEW |
| <i>Sardh</i> | SARDH | Q99LB7 | Sarcosine dehydrogenase, mitochondrial | -2.98 | 1.08 | 4 | Mitochondria | (19, 22, 25-27, 31) |
| <i>Stoml2</i> | STML2 | Q99JB2 | Stomatin-like protein 2 | -3.40 | 1.27 | 1 | Mitochondria | NEW |
| <i>Sucla2</i> | SUCB1 | Q9Z2I9 | Succinyl-CoA ligase [ADP-forming] subunit beta, mitochondrial | 1.19 | -1.35 | 1 | Mitochondria | |
| <i>Acat1</i> | THIL | Q8QZT1 | Acetyl-CoA acetyltransferase, mitochondrial | -3.11 | 1.06 | 1 | Mitochondria | (13-15, 17) |
| <i>Uqcrcf1</i> | UQCRCF1 | Q9CR68 | Cytochrome B-C1 complex subunit Rieske, mitochondrial | -2 | 1 | 1 | Mitochondria | NEW |
| <i>Hnrnpk</i> | HNRPK | P61979 | Heterogenous nuclear ribonucleoprotein K | 2.15 | -1.28 | 3 | mRNA process./translat. | (15) |
| <i>Eif4b</i> | IF4B | Q8BGD9 | Eukaryotic translation initiation factor 4B | 2.14 | -1.37 | 1 | mRNA process./translat. | NEW |
| <i>Rplp0</i> | RLA0 | P14869 | 60S Acidic ribosomal protein P0 | 1.43 | -1.07 | 1 | mRNA process./translat. | (28) |
| <i>Ruvb12</i> | RUVB2 | Q9WTM5 | RuvB-like 2 | 7.28 | -1.1 | 1 | mRNA process./translat. | (16) |
| <i>Hars1</i> | SYHC | Q61035 | Histidyl-tRNA synthetase, cytoplasmic | 2.35 | 1.18 | 1 | mRNA process./translat. | NEW |
| <i>Gars1</i> | SYG | P41250 | Glycyl-tRNA synthetase | 2.43 | 1.09 | 1 | mRNA process./translat. | (15) |
| <i>Wdr12</i> | WDR12 | Q9JJA4 | Ribosome biogenesis protein WDR12 | 2.85 | -1.16 | 1 | mRNA process./translat. | NEW |
| <i>Abhd14b</i> | ABHEB | Q8VCR7 | α/β Hydrolase domain-containing protein 14B | -2.34 | -1.15 | 1 | Not classified | (17, 25, 31) |
| <i>Crtap</i> | CRTAP | Q9CYD3 | Cartilage-associated protein | -3.09 | 1.9 | 1 | Not classified | NEW |
| <i>Ejhd2</i> | EFHD2 | Q9D8Y0 | EF-Hand domain-containing protein D2 | 2.35 | -1 | 1 | Not classified | NEW |
| <i>Ahsg</i> | FETUA | P29699 | Alpha-2-HS-glycoprotein | 4.27 | -1.08 | 1 | Not classified | NEW |
| <i>H2-K1</i> | HA1B | P01901 | H-2 Class I histocompatibility antigen, K-B α chain | -3.09 | 1.9 | 1 | Not classified | NEW |
| N/A | IGHA | P01878 | Ig Alpha chain C region | 2.02 | -1.01 | 1 | Not classified | NEW |
| <i>Iigp1</i> | IIGP1 | Q9QZ85 | Interferon-inducible GTPase 1 | 1.59 | -1.17 | 1 | Not classified | |
| <i>Gaa</i> | LYAG | P70699 | Lysosomal alpha-glucosidase | 2.5 | -1.42 | 1 | Not classified | (17) |
| <i>Kat6a</i> | MYST3 | Q8BZ21 | Histone acetyltransferase KAT6A or MYST3 | 3 | -1.14 | 1 | Not classified | NEW |
| <i>Pebp1</i> | PEBP1 | P70296 | Phosphatidylethanolamine-binding protein 1 | 1.51 | -1.15 | 1 | Not classified | (25) |
| <i>Rgn</i> | RGN | Q64374 | Regucalcin | -5.14 | 1.03 | 3 | Not classified | (13, 15, 22, 25, 31, 32) |
| <i>Rgn</i> | RGN | Q64374 | Regucalcin | 8.4 | -1.18 | 1 | Not classified | (19) |
| <i>Gdi1</i> | GDIA | P50396 | Rab GDP dissociation inhibitor alpha | 2.09 | -1.2 | 2 | Receptor linked | NEW |
| <i>Gdi2</i> | GDIB | Q61598 | Rab GDP dissociation inhibitor beta | 1.52 | -1.19 | 1 | Receptor linked | NEW |
| <i>Atp6v1a</i> | VATA | P50516 | V-Type proton ATPase catalytic subunit A | 5.52 | 1.22 | 1 | Receptor linked | NEW |
| <i>Atp6v1b2</i> | VATB2 | P62814 | V-Type proton ATPase subunit B, brain isoform | 2.35 | 1.18 | 1 | Receptor linked | NEW |
| <i>Cat</i> | CATA | P24270 | Catalase | -2.19 | -1.07 | 2 | Redox regulation | (13-15, 20, 22, 32) |
| <i>Dhdh</i> | DHDH | Q9DBB8 | Trans-1,2-dihydrobenzene-1,2-diol dehydrogenase | -1.4 | -1.33 | 1 | Redox regulation | (15) |
| <i>Gpx1</i> | GPX1 | P11352 | Glutathione peroxidase 1 | -1.98 | -1.10 | 3 | Redox regulation | (15, 25, 31) |
| <i>Grhpr</i> | GRHPR | Q91Z53 | Glyoxylate reductase/hydroxy-pyruvate reductase | 1.7 | -1.14 | 1 | Redox regulation | Conflict (26) |
| <i>Prdx2</i> | PRDX2 | Q61171 | Peroxioredoxin 2 | 1.51 | -1.15 | 1 | Redox regulation | (24, 25) |

Table I. Continued

Table I. *Continued*

| Gene name | UniProtKB name | Accession number | Full protein name | Average ratio | | Number of spots | Functional classes GO annotation | Reference |
|-----------------|----------------|------------------|--|---------------|-------|-----------------|----------------------------------|----------------------|
| | | | | HCC/KO | KO/WT | | | |
| <i>Alb</i> | ALBU | P07724 | Serum albumin | 4.94 | -1.32 | 22 | Transport | (14, 22, 26, 27, 31) |
| <i>Ehd4</i> | EHD4 | Q9EQP2 | EH domain-containing protein 4 | -1.2 | -1.33 | 1 | Transport | |
| <i>Hpx</i> | HEMO | Q91X72 | Hemopexin | 2.93 | -1.15 | 5 | Transport | (25) |
| <i>Selenbp1</i> | SELENBP1 | P17563 | Methanethiol oxidase/selenium-binding protein 1 | 3.60 | -1.06 | 2 | Transport | (19) |
| <i>Snx6</i> | SNX6 | Q6P8X1 | Sorting nexin-6 | 1.59 | -1.17 | 1 | Transport | |
| <i>Tg</i> | THYG | O08710 | Thyroglobulin | -5.74 | 1.17 | 1 | Transport | NEW |
| <i>Tf</i> | TRFE | Q92111 | Serotransferrin | -1.5 | -1.01 | 1 | Transport | (13, 32) |
| <i>Tf</i> | TRFE | Q92111 | Serotransferrin | 5.92 | 1.52 | 1 | Transport | (15, 22, 26, 31) |
| <i>Gc</i> | VTDB | P21614 | Vitamin D-binding protein | 4.27 | -1.08 | 1 | Transport | (22) |
| <i>Cops4</i> | CSN4 | O88544 | COP9 Signalosome complex subunit 4 | 4 | 1.05 | 1 | Ubiquitination/ degradation | NEW |
| <i>Psmc4</i> | PRS6B | P54775 | 26S Proteasome regulatory subunit 6B | 3.69 | -1.28 | 1 | Ubiquitination/ degradation | NEW |
| <i>Psmc2</i> | PRS7 | P46471 | 26S Proteasome regulatory subunit 7 | 1.52 | -1.19 | 1 | Ubiquitination/ degradation | NEW |
| <i>Psm13</i> | PSD13 | Q9WVJ2 | 26S Proteasome non-ATPase regulatory subunit 13 | 1.50 | -1.06 | 1 | Ubiquitination/ degradation | NEW |
| <i>Psmb4</i> | PSMB4 | P99026 | Proteasome subunit beta type 4 | 1.97 | 1 | 1 | Ubiquitination/ degradation | (31) |
| <i>Uba1</i> | UBA1 | Q02053 | Ubiquitin-like modifier-activating enzyme 1 | 3.63 | -1.14 | 2 | Ubiquitination/ degradation | NEW |

KO: Knockout; WT: wild-type; HCC: hepatocellular carcinoma tissue.

1/1,000; Cell Signaling Technology); monoclonal mouse anti-phospho-MYC S62 (dilution 1/500; BioAcademia, Osaka, Japan), rabbit polyclonal anti-phospho-mTOR S2448 (dilution 1/500; Cell Signaling Technology); mouse monoclonal anti-phospho-p70 S6K T389 (dilution 1/1,000; Cell Signaling Technology); and rabbit polyclonal anti-GLI family zinc finger 1 (GLI1) (dilution 1/500; Santa Cruz Biotechnologies). Incubation with horseradish peroxidase-conjugated secondary antibodies (dilution 1/5,000; Cell Signaling Technology) was performed for 1h at 4°C. To visualize the bands, the blots were developed on an ImageQuant LAS 4000 system (GE Healthcare) using Western Bright ECL detection kit (Advansta, San Jose, CA, USA). All densitometric quantifications were carried out with ImageJ software (Imagej.net/ImageJ). An unpaired two-tailed *t*-test was used for statistical analysis and *p*-values below 0.05 were considered significant.

Bioinformatics. The complete dataset of differentially expressed/regulated proteins was loaded into the Ingenuity Pathway Analysis (IPA) software (IPA version 8.7) and database (Ingenuity Systems, Redwood City, CA, USA) to find the most relevant canonical pathways, toxicity pathways or biological functions.

Results

Histopathological and molecular description of murine liver samples used for proteomics analysis. Four independent HCC samples from four randomly chosen *Ppp2r5d* KO mice

exhibiting spontaneous hepatocarcinogenesis were collected and snap-frozen, together with a non-cancerous sample from the same livers (paired analysis). The pathological state of the frozen samples, side-by-side with a paraformaldehyde-fixed and hematoxylin/eosin-stained sample of the same tissues (Figure 1A), was confirmed by an experienced liver pathologist. Normal liver tissues from four age- and gender-matched WT mice (19m, 21m, 22m and 23m) were additionally collected as reference tissues. Although ranging from well- to poorly differentiated, all HCC samples showed increased c-MYC Ser62 phosphorylation, but differed in the activation of other oncogenic pathways, including MEK/ERK, mTOR/p70 S6K and Hedgehog signaling, as previously reported (36) (Figure 1B). One HCC sample showed 'pale body'-like structures of unknown significance (Figure 1A).

Comparative 2D-DIGE analysis. We next generated protein-expression profiles of the protein lysates of these WT liver (n=4), KO HCC (n=4) and KO non-tumor tissues (n=4) using 2D-DIGE. For this purpose, an internal standard was created, in which 25 µg of each lysate (n=12) was mixed, and labelled with Cy2. Two WT, two KO tumor and two KO non-tumor tissue lysates were labelled with Cy3; the remaining two WT,

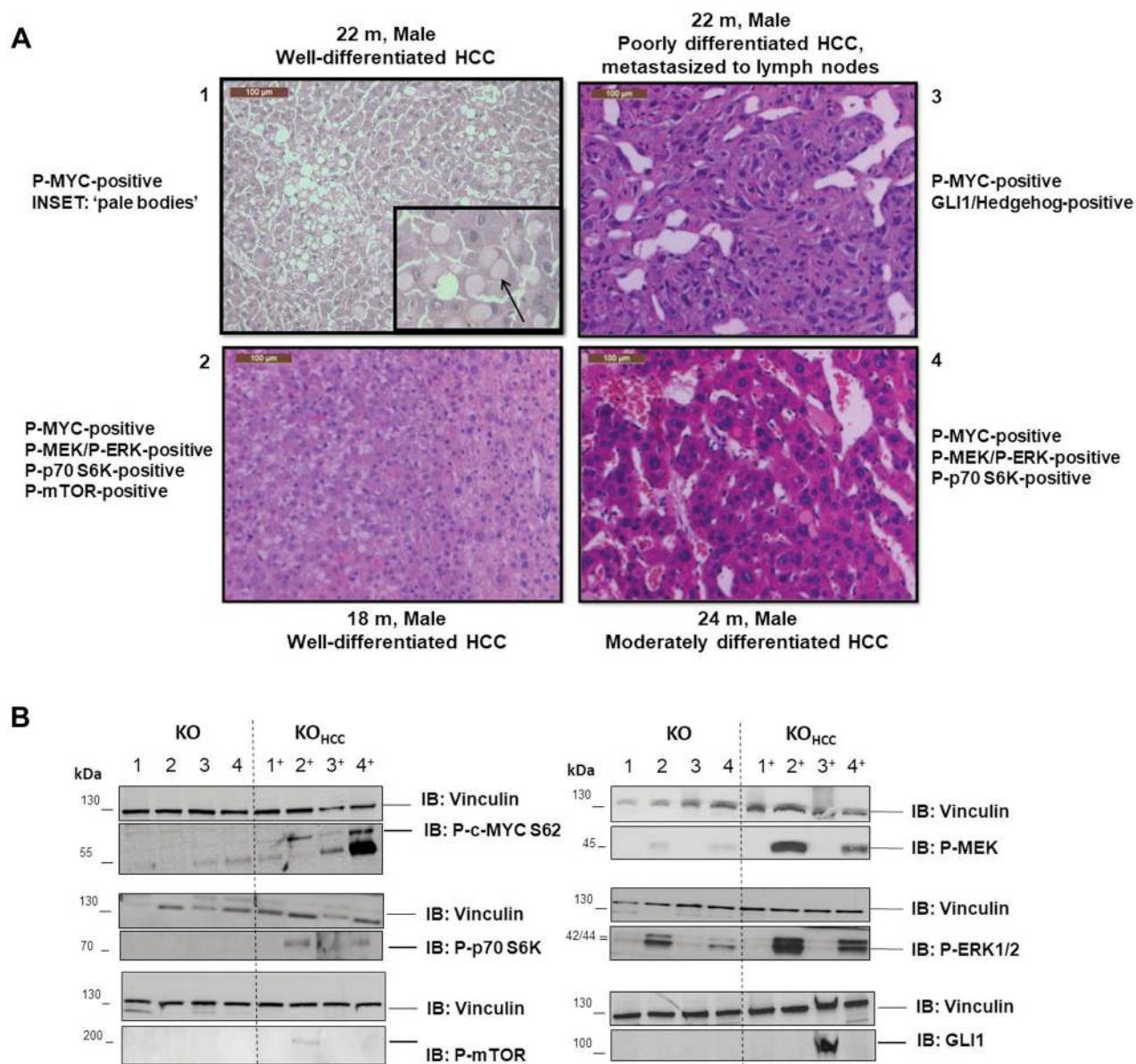


Figure 1. Histopathology of murine protein phosphatase 2A regulatory subunit B56 δ (Ppp2r5d) knockout (KO) hepatocellular carcinoma (HCC) samples used for proteomics analysis. A: Hematoxylin/eosin-stained sections of the analyzed HCC tissues (n=4) were evaluated by an experienced liver pathologist, and diagnosed as well-differentiated (samples 1 and 2), moderately differentiated (sample 4) and poorly differentiated (sample 3). The latter tumor had been metastasized to the lymph nodes and was positive for expression of the GLI family zinc finger 1 (GLI1) Hedgehog signaling transcription factor. Sample 1 showed 'pale bodies' (arrow in inset) of unknown significance. All scale bars: 100 μ m. B: Immunoblotting analysis with indicated antibodies of the upper HCC samples and adjacent non-cancerous liver samples of the same mice (paired analysis) showed sporadic activation of MAP-extracellular signal-regulated kinase (MEK)/extracellular signal-regulated kinase (ERK), mammalian target of rapamycin (mTOR)/p70 ribosomal protein S6 kinase (p70 S6K) and Hedgehog signaling, while c-MYC S62 phosphorylation was up-regulated in all HCC samples analyzed.

two KO tumor and two KO non-tumor lysates were labelled with Cy5. By normalizing the Cy3 or Cy5 intensities to the Cy2 control, it was possible to compensate for gel-to-gel variations. Direct comparison between Cy3 and Cy5 spot

intensities allowed identification of differentially expressed or regulated proteins. All samples were first resolved on six gels with isoelectric focusing in pH range 4-7, and then re-run on another six gels with isoelectric focusing in pH range

6-9. In pH range 4-7, 22 differentially expressed spots were detected between WT and non-cancerous KO liver samples ($p < 0.05$), and 154 differentially expressed spots were identified between KO HCC and KO non-tumor tissue ($p < 0.05$) (Figure 2A). In pH range 6-9, seven spots for differentially expressed proteins between WT and non-cancerous KO livers were found ($p < 0.05$), while 58 were identified between KO HCC and KO non-tumor tissue ($p < 0.05$) (Figure 2A). Representative examples of the analysis of spots that were up-regulated and down-regulated, respectively, in KO HCC are shown (Figure 2B).

MS-based protein identification. Subsequent MS analysis by MALDI TOF/TOF of the spots of differentially regulated proteins eventually resulted in the identification of 129 differentially expressed proteins between either or both conditions (Table I). Twenty proteins were down-regulated in non-tumor KO compared with WT livers, while only three proteins were up-regulated in non-tumor KO *versus* WT livers. Moreover, the fold-changes in expression between these samples were relatively small, ranging between 1.17- to 1.46-fold down-regulation, and between 1.66- to 1.71-fold up-regulation (Table I).

In contrast, many more proteins were found to be differentially expressed between KO HCC and KO non-tumor samples, with much higher absolute differences: 43 were down-regulated in the tumors (range=1.1- to 5.74-fold), while 80 proteins were up-regulated in the tumors (range=1.43- to 35.28-fold) (Table I). Interestingly, four proteins (tubulin alpha-1A chain, METK1, regucalcin and serotransferrin) showed apparently conflicting differential expression patterns in HCC *versus* non-tumor KO tissues, as they were found to be both up-regulated as well as down-regulated in the tumors (Table I). This might imply they may actually occur as different protein isoforms, for instance due to differing post-translational modifications or protein processing events. Hence, a total of 119 proteins showed different expression or regulation in normal KO liver *versus* HCC KO liver, and were denoted as 'cancer proteins'. Based on Gene Ontology (GO) annotations, these cancer proteins can be grouped into 14 functional classes, covering a wide spectrum of biological functions (Table I and Figure 3). Notably, almost one-quarter of the cancer proteins (23%) belonged to 'liver metabolism' (n=22) or 'glucose metabolism' (n=6), and appeared mostly to be down-regulated in the tumors, consistent with a degree of hepatocyte de-differentiation and altered cancer cell metabolism. Another 18% of the cancer proteins were functionally associated with 'mitochondria' (mostly down-regulated in the tumors), and 15% with 'cytoskeleton' (mostly up-regulated in the tumors). Other functional classes were related to 'cell cycle', 'endoplasmic reticulum/protein folding', 'lipid metabolism', 'mRNA processing/translation', 'transport' and 'protein ubiquitination/degradation' (all predominantly up-

regulated in the tumors) (Figure 3). Interestingly, 66 (56%) cancer proteins had previously been identified in other proteomic studies of HCC samples from patients, mice or rats (Table I, last column), while the remaining 55 (44%) others may represent potentially new HCC biomarkers (Table I, last column, 'NEW'). Four proteins of the latter group had however been reported as differentially regulated in HCC in at least one other study, but in the opposite direction of what we found here, potentially testifying once more to the presence of differentially modified proteins rather than differential expression (Table I, last column, 'conflict').

Comparison between 'cancer proteins' and 'cancer genes'. We compared the differentially expressed proteins between KO HCC and KO non-cancerous samples identified here with the differentially expressed genes previously determined by RNAseq analysis in a similar set of *Ppp2r5d* KO mouse samples (36). Intriguingly, we found the overlap between both datasets was overall rather poor: of 29 differentially expressed genes between WT and KO samples (36), none overlapped with the 23 differentially regulated proteins identified here; and, of 351 differentially expressed genes between KO non-tumor and KO HCC samples (36), only 14 were also retrieved in the list of 119 differentially regulated proteins (Figure 4). For these 14 genes/proteins, the changes in expression were fully concordant at the mRNA and the protein level.

IPA-assisted pathway analysis of differentially regulated proteins. The cancer protein dataset was subsequently loaded into the IPA software and database (IPA; Ingenuity Systems) to identify links with the most relevant functional pathways or altered molecular networks. Importantly, the results confirm the diagnosis of HCC at the biochemical level, since 'cancer' and 'gastrointestinal disease' were the two top hits (Figure 5). Within the top altered pathways and molecular/cellular functions, several metabolic pathways were identified, including amino acid metabolism and the urea cycle, and methionine metabolism. Thus, this analysis indirectly confirms the quality and biological relevance of data obtained by the 2D-DIGE proteomics technique.

Validation of select differentially regulated proteins. One of the most up-regulated proteins in the HCCs was fibrinogen gamma (7.28-fold higher *versus* adjacent non-tumor tissue) (Table I). A closer inspection of the data revealed, however, that this up-regulation predominantly occurred in one of the four HCC samples analyzed, coinciding with the appearance of the 'pale body' structures identified during histopathological examination (Figure 1A). Additional electron microscopy examination of the 'pale bodies' showed rounded dilated cisternae of the rough endoplasmic reticulum (RER), containing amorphous, granular material (Figure 6A), most likely representing fibrinogen deposits. Fibrinogen is a protein

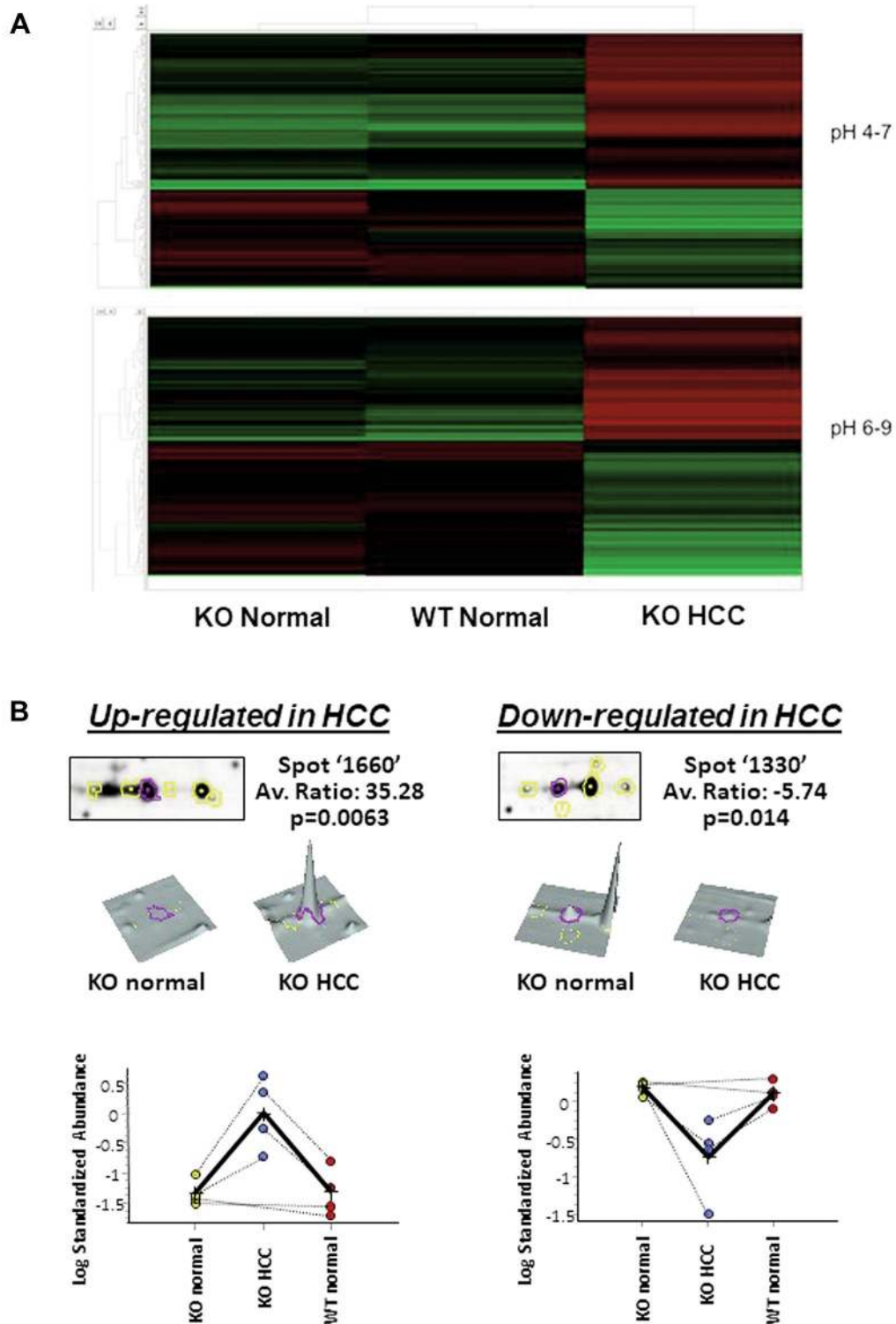


Figure 2. Analysis of differentially regulated spots following two-dimensional differential gel electrophoresis (2D-DIGE) A: Cluster analysis of differentially regulated 'spots' between wild-type (WT), protein phosphatase 2A regulatory B56 δ subunit (Ppp2r5d) knockout (KO) non-cancerous, and Ppp2r5d KO hepatocellular carcinoma (HCC) liver tissue, grouped by pH range. Red: up-regulated; green: down-regulated. B: Examples of spot picking and analysis using DeCyder V 7.0 software, for typically up-regulated (left) and down-regulated (right) spots in the KO HCC samples. Proteins in spots were accepted as being differentially expressed when showing a statistically significant ($p < 0.05$) increase or decrease when compared to the control in at least 75% of the spot maps.

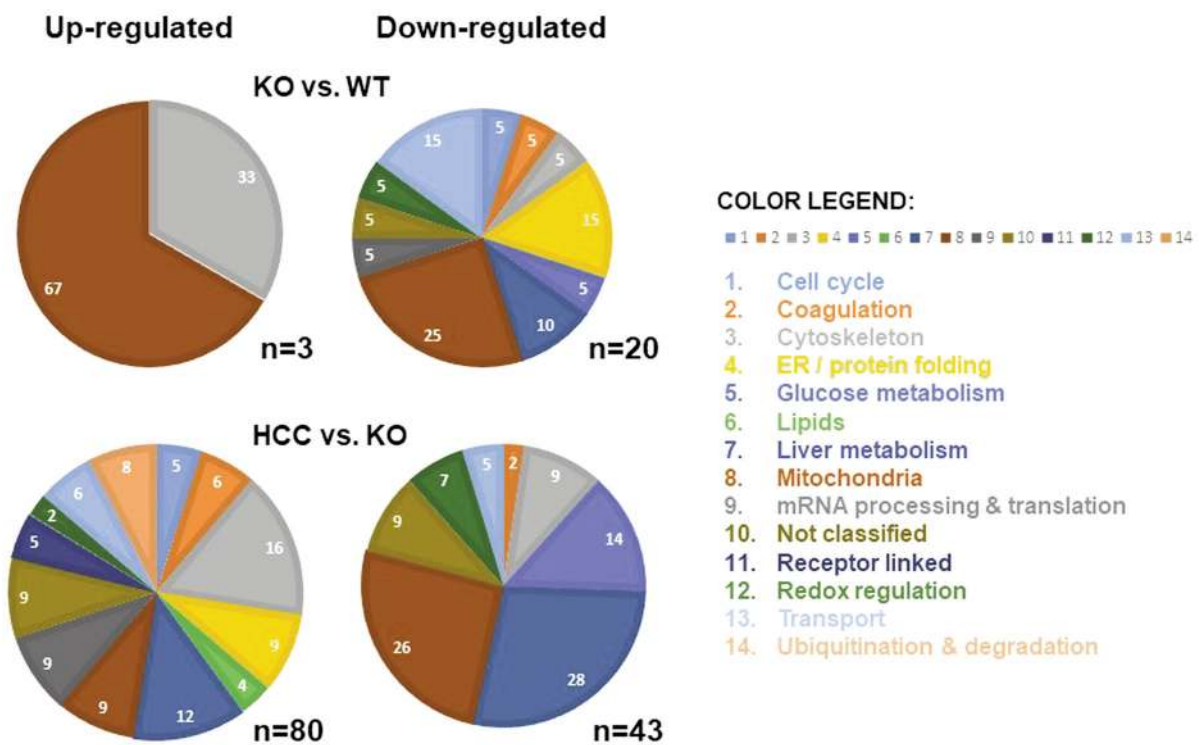


Figure 3. Overview of differentially regulated proteins, grouped into 14 functional classes based on Gene Ontology (GO) annotation. *n*: Absolute number of up-regulated or down-regulated proteins found; the numbers within the diagrams indicate percentages. In the hepatocellular carcinoma (HCC) samples, the most frequently altered proteins belonged to liver metabolism (28% of those down-regulated in HCC, and 12% of those up-regulated in HCC), mitochondria (26% of those down-regulated in HCC, and 9% of those up-regulated in HCC), glucose metabolism (14% of those down-regulated in HCC) and cytoskeleton (16% of those up-regulated in HCC, and 9% of those down-regulated in HCC).

synthesized exclusively by hepatocytes, and the intracellular deposition might reflect an impairment in its transport and/or secretion. Interestingly, such fibrinogen deposits have also been reported in human HCCs in 5-5.7% of cases, depending on the study (47, 48). In the B56 δ KO mice, the overall incidence of pale body occurrence was 12% (3/25, $n=25$) (Figure 6B), matching well with the human HCC data.

Additional validation of the differential proteomics results was performed by western blot analysis of a select number of identified proteins for which antibodies were available. Consistent with the 2D-DIGE results (Table I), down-regulation of FBP1 was observed in all HCC samples (Figure 6C). Interestingly, this protein is also down-regulated in human HCC and was suggested to be one of five potential HCC biomarkers identified from a meta-analysis of several proteomic HCC profiling studies (49). In contrast, the slightly increased expression of the PP2A scaffolding A subunit (Table I) was not confirmed by immunoblotting (Figure 6C), suggesting it might rather represent a difference in post-translational modification of this protein. Supporting this hypothesis is another 2D-DIGE study which identified

an opposite change in PP2A A subunit expression in HCC, *i.e.* down-regulation, neither confirming this by western blotting (25). Immunoblots further confirmed the down-regulation of phosphoglucomutase-2 (PGM2) (Figure 6C). For *S*-adenosyl methionine synthase 1 (METK1), immunoblots confirmed significant down-regulation (Figure 6C), in concordance with the mRNA expression data (Figure 4). However, the 2D-DIGE data additionally identified a spot of this protein significantly up-regulated in the HCCs (7.28-fold, $p>0.05$; Table I), suggestive of potential post-translational modification(s) of METK1 in the tumors.

Discussion

Genomic and mRNA analyses of human and mouse HCC have revealed significant overlaps between chromosomal aberrations and gene-expression signatures (50). However, because proteins rather than mRNA are the major effectors of cellular and tissue functions, complementary comparative analyses at the proteome level are equally important in gaining insights into the mechanisms of hepatocarcinogenesis

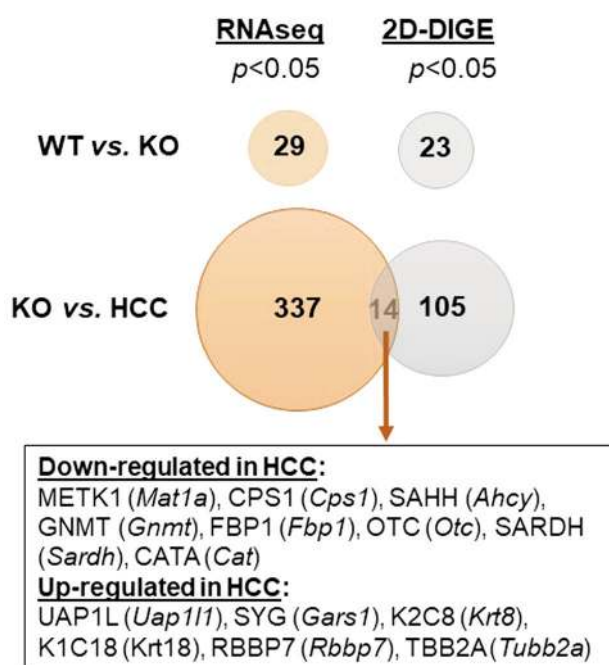


Figure 4. Comparison between the number of differentially expressed mRNAs as determined by RNAseq (36) and as identified in the current study. While there was no overlap between both datasets in the livers from wild-type (WT) vs. non-cancerous knockout (KO) mice, 14 genes/proteins appeared to be commonly regulated at the mRNA and protein levels in the non-cancerous KO livers vs. the KO HCCs. The identities of these ‘cancer’ genes/proteins are detailed in the box.

and to discover novel prognostic or predictive markers for improved HCC (targeted) treatment. Here, we used 2D-DIGE to identify changes between the proteome of spontaneous HCCs in *Ppp2r5d* KO mice, their surrounding non-tumoral tissue and normal WT liver tissue. We identified 23 proteins differentially expressed or regulated between normal WT and KO livers, and 119 proteins differentially expressed or regulated between KO HCC and normal KO livers (the latter defined as ‘cancer proteins’). Intriguingly, the overlap with our previously published transcriptomics data, performed on mRNA isolated from similar tissue samples, was very poor, with only 14 proteins/mRNAs commonly found differentially expressed between KO HCC and non-tumor KO tissue, and thus, only 12% of the cancer proteins concordantly regulated at the mRNA level. It is known that proteins with very high or very low pI as well as hydrophobic proteins are in general more difficult to detect by 2D-DIGE, and that there is some bias in favor of cytoplasmic and soluble proteins (18). Moreover, 2D-DIGE is definitely biased towards the identification of medium to highly abundant proteins and does not provide a comprehensive nor representative view of

IPA Summary of Analysis

| Top networks | | score: |
|--|--|------------------------|
| 1 | Small molecule biochemistry, cancer, reproductive system disease | 55 |
| 2 | Immunological disease, hematological disease, inflammatory disease | 46 |
| 3 | Cellular compromise, organismal injury, abnormalities lipid metabolism | 23 |
| 4 | Lipid metabolism, molecular transport, small molecule biochemistry | 23 |
| 5 | Cell death, tumor morphology, cell-to-cell signaling and interaction | 2 |
| Top bio functions | | number of molecules |
| Diseases and disorders | | |
| 1 | Cancer | 38 (1.7E-09 - 3.0E-02) |
| 2 | Gastrointestinal disease | 22 (1.7E-09 - 3.0E-02) |
| 3 | Hematological disease | 22 (2.5E-09 - 2.5E-02) |
| 4 | Immunological disease | 23 (5.3E-08 - 2.6E-02) |
| 5 | Inflammatory disease | 30 (6.7E-08 - 2.6E-02) |
| Molecular and cellular functions | | |
| 1 | Small molecule biochemistry | 31 (5.8E-08 - 3.3E-02) |
| 2 | Amino acid metabolism | 11 (1.9E-06 - 2.5E-02) |
| 3 | Cellular assembly and organization | 15 (1.7E-05 - 2.9E-02) |
| 4 | Cell morphology | 8 (5.2E-05 - 3.2E-02) |
| 5 | Post-translational modification | 13 (5.2E-05 - 2.9E-02) |
| Physiological system development and function | | |
| 1 | Hair and skin development and function | 4 (1.7E-05 - 2.1E-02) |
| 2 | Organismal development | 9 (1.7E-05 - 3.1E-02) |
| 3 | Hepatic system development and function | 2 (5.2E-05 - 3.0E-02) |
| 4 | Endocrine system development and function | 2 (1.0E-04 - 2.5E-02) |
| 5 | Tissue development | 11 (7.2E-04 - 3.3E-02) |
| Top canonical pathways | | p-Value: |
| 1 | Acute phase response signaling | 7.70E-05 |
| 2 | 14-3-3 Mediated signaling | 1.14E-04 |
| 3 | Urea cycle and metabolism of amino groups | 1.23E-04 |
| 4 | Breast cancer regulation by stathmin 1 | 1.22E-03 |
| 5 | Methionine metabolism | 1.49E-03 |

Figure 5. In silico pathway analysis of ‘cancer proteins’. Ingenuity Pathway Analysis (IPA) of 119 proteins differentially regulated between knockout (KO) hepatocellular carcinoma (HCC) and non-cancerous KO livers, with indication of Top networks, bio-functions and canonical pathways.

the tissue proteome. On the other hand, a change in mRNA level does not always reflect a corresponding change in protein level, especially for proteins with a low turnover. Finally, an obvious difference in protein expression as identified by 2D-DIGE may actually also represent expression of an altered isoform, post-translationally modified or processed form of the protein, which cannot be detected by RNAseq analysis. This all illustrates the complementarity of transcriptomic and proteomic analyses.

Unbiased IPA analysis of the cancer proteins identified ‘gastrointestinal disease’ and ‘cancer’ as the top hits, independently confirming the diagnosis of our samples and hence, indirectly, the quality of the data obtained. In addition, within the cancer proteins, several established HCC biomarkers or differentially expressed proteins identified in former 2D-DIGE studies of human, rat or mouse HCC samples were confirmed (56%) (Table I, indicated in bold), further testifying to the data quality and suitability of the model.

When looking in more detail at the list of cancer proteins, an obvious finding is the overt decrease in ‘metabolism’-associated proteins in the *Ppp2r5d* KO HCCs, both in

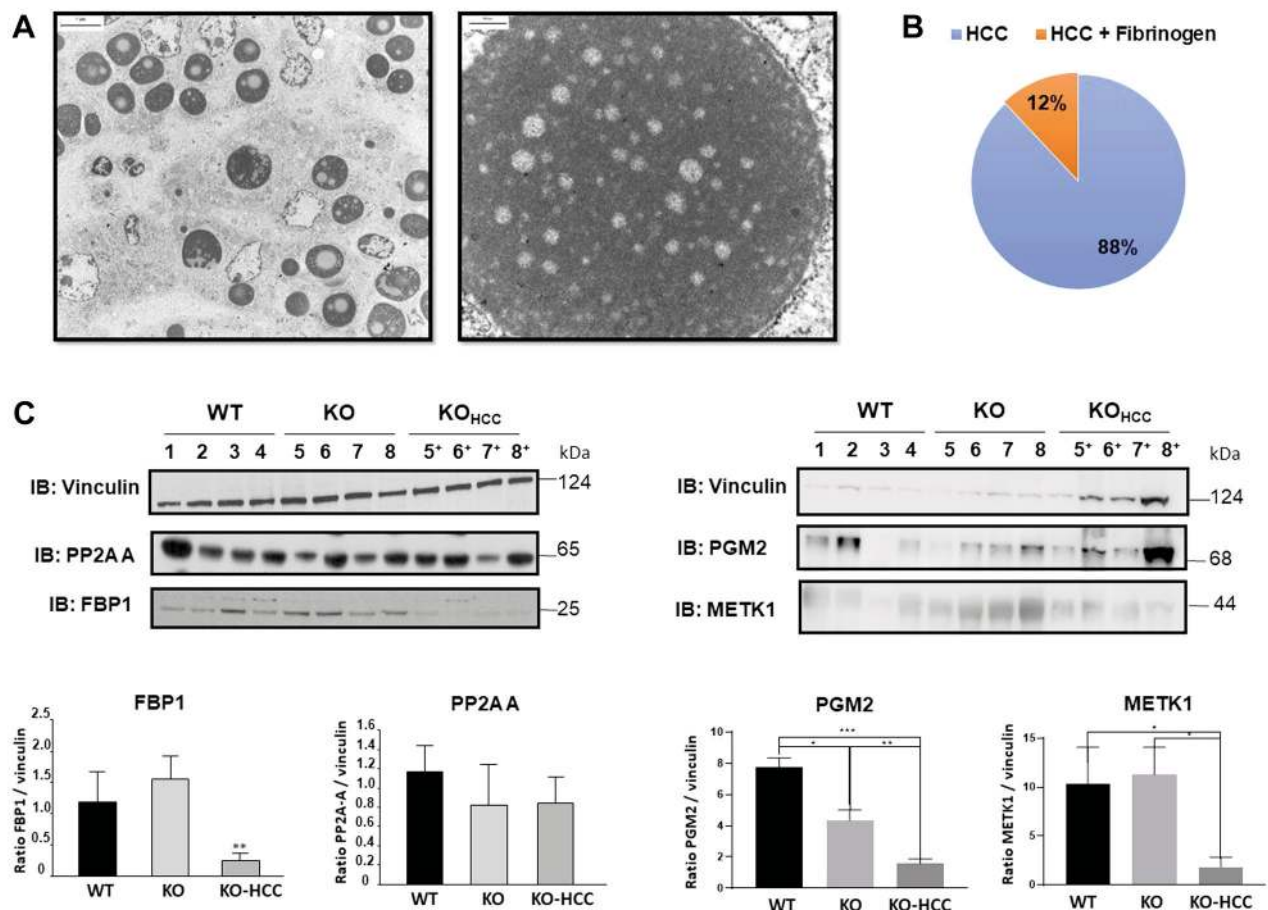


Figure 6. Validation of two-dimensional differential gel electrophoresis (2D-DIGE) results. **A**: Additional analysis of 'pale body' structures by electron microscopy. **B**: Frequency of occurrence of fibrinogen deposits in hepatocellular carcinomas (HCCs) from protein phosphatase 2A (PP2A) regulatory B56 δ subunit (Ppp2r5d) knockout (KO) mice. Total number of hepatocellular carcinomas (HCCs) analyzed was 25. **C**: Validation of differentially expressed/regulated proteins by immunoblotting. FBP1 (fructose-1,6-bisphosphatase 1): 4.7-fold less expression in HCC compared to wild-type (WT) ($p=0.015$) and 6.2-fold less expression compared to non-tumor KO ($p=0.002$). PP2A scaffolding A subunit: no significant differences in expression between HCC, non-tumor KO or WT ($p>0.05$). Phosphoglucomutase-2 (PGM2): 5.5-fold less expression in HCC compared to WT ($p=0.0001$) and 3.3-fold less expression compared to non-tumor KO ($p=0.0086$). S-Adenosylmethionine synthase 1 (METK1): 5.7-fold less expression in HCC compared to WT ($p=0.049$) and 6.1-fold less expression compared to non-tumor KO ($p=0.019$).

proteins classified as belonging to 'glucose metabolism' as 'liver metabolism' – not only testifying to significant metabolic changes in the cancer cells, but likely also to a degree of de-differentiation of the hepatocytes. Down-regulation of *Fbp1* (an enzyme promoting gluconeogenesis), seen at the mRNA level as well (Figure 4) and confirmed by immunoblotting (Figure 6B), suggests changes in glucose metabolism consistent with the Warburg effect (a change from oxidative phosphorylation to aerobic glycolysis) (51). Several enzymes involved in protein and amino acid degradation [e.g. phenylalanine-4-hydroxylase (PH4H), mitochondrial acetyl-CoA acetyltransferase (THIL), cytoplasmic malate dehydrogenase (MDHC)] were also

reduced, while proteins involved in glutamine (a critical amino acid for proliferation of tumor cells) synthesis were up-regulated [e.g. ornithine aminotransferase (OAT)] as well as proteins involved in protein translation in general [e.g. eukaryotic translation initiation factor 4B (IF4B), 60S acidic ribosomal protein P0 (RLA0), histidyl-tRNA synthetase (SYHC), glycyl-tRNA synthetase (SYG), ribosome biogenesis protein WDR12 (WDR12)] and in protein maturation processing [e.g. methionine aminopeptidase 1D (AMP1D), protein disulfide-isomerase (PDIA1), protein disulfide-isomerase A3 (PDIA3)] (Table I). The urea cycle seemed significantly impaired in the HCCs [e.g. down-regulation of carbamoyl-phosphate synthase (CPS1) and

ornithine carbamoyl transferase (OTC)] as was the liver methylation cycle, with four essential enzymes in this process, METK1, glycine *N*-methyl transferase (GNMT), betaine-homocysteine-*S*-methyl transferase 1 (BHMT1) and adenosyl homocysteinase (SAHH), all being down-regulated (Table I). Down-regulation of METK1, validated by our immunoblotting results (Figure 6B), and down-regulation of SAHH and GNMT are likely caused by reduced gene expression, as *Mat1a*, *Ahcy* and *Gnmt* mRNAs were also found to be reduced in the ‘cancer genes’ list (Figure 4) (36). Interestingly, however, we also found METK1 to be significantly up-regulated in a different spot (Table I), likely testifying from a different post-translationally modified form or different isoform, being specifically increased in the HCCs. Such explanation would also reconcile seemingly contradicting data in literature, describing *METK1* up-regulation (12, 31), as well as down-regulation in HCC (13, 14). In any case, down-regulation of the methylation cycle and, hence, chronic *S*-adenosyl-*L*-methionine deficiency, have been shown to result in spontaneous HCC development in *Mat1a* and *Gnmt* KO mice (52, 53), which our data are fully consistent with.

A similar explanation may hold true for tubulin alpha-1A chain (TBA1A), serotransferrin (TRFE) and regucalcin (RGN), which we and others (Table I) identified in inversely altered spots, seemingly both up-regulated and down-regulated in HCC. RGN is a senescence marker, suppresses HCC growth *in vitro* (54, 55) and its expression is correlated with improved survival of patients with HCC (54), suggesting it is likely expressed less in the *Ppp2r5d* KO HCCs, while the spot of up-regulated protein may represent a modified form. In contrast, TBA1A is a cytoskeletal protein that was likely up-regulated in the *Ppp2r5d* KO HCCs, as was the case for at least three other members of the tubulin family that were differentially regulated in our dataset (TBB2A, TBB2B, TBB5; Table I); and TBB2A also at the mRNA level (Figure 4) alongside several other cytoskeleton proteins (different cytokeratins, desmin and vimentin). Vimentin is known to be abundantly expressed in human HCC and its overexpression is significantly associated with HCC metastasis (56). Likewise, expression levels of cytokeratin 8 (K2C8) have been positively correlated with HCC metastatic ability (57), and this up-regulation apparently occurs at the mRNA level (Figure 4). Together with serum albumin and apolipoprotein A1, serotransferrin was amongst the most highly up-regulated proteins in the cancer protein list. We suggest that the huge increase of these proteins in HCCs might actually represent accumulation of extravascular plasma protein in the tumor microenvironment, and not necessarily increased protein synthesis by the tumor cells. Increased serotransferrin levels in that environment might additionally induce transferrin-mediated iron uptake, thereby satisfying the high iron demand of the highly proliferating cancer cells. The spot

representing down-regulated serotransferrin may again correspond to an altered post-translationally modified form or transferrin isoform.

Equally highly overexpressed in the HCCs was fibrinogen- γ . Fibrinogen is a protein exclusively synthesized by hepatocytes, and it was specifically found to be overexpressed in one of four HCC samples analyzed, which at the histological level featured ‘pale body’ structures (Figure 1A), and at the ultrastructural level appeared as dilated cisternae of the RER, filled with amorphous, granular material (Figure 6A). Since the RER is the site of protein synthesis, and fibrinogen is a secreted protein, its retention in the RER likely represents deficient translocation to the smooth ER or Golgi apparatus, and eventually a defect in fibrinogen transport. Interestingly, such pale bodies are observed in about 5-5.7% of human HCCs (47, 48) and therefore represent another clinical feature of *Ppp2r5d* (B56 δ) KO HCC that we found in 12% of our analyzed mouse HCC samples.

The down-regulation of mitochondrial proteins, except mitochondrial heat-shock proteins (HSPs), which were significantly up-regulated, suggest a loss of function of this organelle, with potentially increased stress. The up-regulation of several molecular chaperones [mitochondrial stress-70 protein (GRP75), 78 kDa glucose-regulated protein (GRP78), heat-shock cognate 71 kDa protein (HSP7C) and mitochondrial 60 kDa heat-shock protein (CH60)] has been reported in several HCC studies (Table I), and the overexpression of these proteins may be interpreted as a response to the stressful cancerous environment for cytoprotective functions. Up-regulation of HSPs may also contribute to the tumor cell adaptive response to altered oxygen levels, as testified by altered expression of antioxidant defense enzymes, such as catalase (CATA), glutathione peroxidases (GPX1) and peroxiredoxins (PRDX2) (Table I).

The HCCs also showed an increased protein ubiquitination/degradation signature, with upregulation of proteins belonging to the ubiquitin-mediated degradation machinery [*e.g.* 26S protease regulatory subunit 6B (PRS6B), 26S protease regulatory subunit 7 (PRS7), 26S proteasome non-ATPase regulatory subunit 13 (PSD13) and proteasome subunit beta type 4 (PSMB4)], as well as of proteins enzymatically regulating the poly-ubiquitination process [*e.g.* ubiquitin-like modifier-activating enzyme 1 (UBA1)]. Increased ubiquitin immunopositivity has also been observed in human HCC samples, and was predictive for HCC re-occurrence (58).

Thus, as a first conclusion, our study confirmed many of previously found protein HCC biomarkers. Such a successful reproduction of previously reported results clearly underscores the applicability of the approach. Moreover, it demonstrates the suitability of spontaneous HCC development in *Ppp2r5d* KO mice as a new valuable murine hepatocarcinogenesis model that captures many characteristics of the human disease.

In addition, however, our study also identified many previously unreported molecules that might theoretically have significant roles in HCC tumorigenesis or progression and become novel HCC biomarkers (Table I, last column, 'NEW'). For us, the most suitable candidates for further validation seem to be the three proteins categorized as 'cell cycle' proteins [coiled-coiled domain protein 15 (CCDC15), protein ELYS (ELYS) and histone-binding protein RBBP7 (RBBP7)], which were all significantly up-regulated in the HCCs (2.51- to 4.92-fold); the cytoskeletal protein desmin (3.51-fold up-regulated); phosphoglucosyltransferase-2 (PGM2) (2.95-fold down-regulated, confirmed by immunoblotting); several liver metabolic enzymes [*e.g.* adipocyte plasma-membrane associated protein (APMAP) and guanine deaminase (GUAD), 3.44- and 3.09-fold down-regulated]; several mitochondrial enzymes, particularly NADH dehydrogenase flavoprotein 2 (35.28-fold up-regulated); eIF4B and WDR12 (up-regulated 2.14- and 2.85-fold); receptor-linked proteins Rab GDP dissociation inhibitor alpha (GDIA), GDIB, V-type protein ATPase catalytic subunit A (VATA) and VATB2 (up-regulated 1.52- to 5.52-fold); thyroglobulin (5.74-fold down-regulated); protein degradation-linked proteins COP9 signalosome complex subunit 4 (CSN4), UBA1 and PRS6B (4-, 3.63- and 3.69-fold up-regulated); and some 'unclassified proteins' (*e.g.* histone acetyltransferase MYST3, 3-fold up-regulated). Further validation and investigation of these proteins in human HCC samples may eventually result in the discovery of new molecular targets for therapy, or biomarkers for early detection or prognosis.

Conflicts of Interest

The Authors have no conflicts of interest to declare.

Authors' Contributions

C.L. performed all mouse-related experiments, tissue isolation, protein extraction, MS sample preparation and overall data analysis; G.B.F. performed 2D gel electrophoresis and 2D-DIGE-related data analysis (spot picking; clustering); J.D.O. performed and analyzed immunoblot validation experiments; L.L. performed histopathologic analysis of all liver tissues; R.D.V. performed electron microscopy; R.D. analyzed data by IPA software; L.O. and C.M. supervised 2D-DIGE analysis; E.W. performed MS analysis and data processing (Mascot search and protein identifications); VJ and EW designed and supervised the study, and wrote the article.

Acknowledgements

Funding was provided by the KU Leuven Research Fund (C24/17/073 to V.J. and R.D.), the Belgian IAP program (P7/13 to V.J. and E.W.), the Research Foundation-Flanders (G.0B01.16N to V.J.; FWO-SB fellowship to J.D.O.) and the Flemish Agency for Innovation by Science and Technology (IWT-SB fellowship to C.L.).

References

- Torre LA, Bray F, Siegel RL, Ferlay J, Lortet-Tieulent J and Jemal A: Global cancer statistics, 2012. *CA Cancer J Clin* 65(2): 87-108, 2015. PMID: 25651787. DOI: 10.3322/caac.21262
- Llovet JM, Montal R, Sia D and Finn RS: Molecular therapies and precision medicine for hepatocellular carcinoma. *Nat Rev Clin Oncol* 15(10): 599-616, 2018. PMID: 30061739. DOI: 10.1038/s41571-018-0073-4
- Bruix J, da Fonseca LG and Reig M: Insights into the success and failure of systemic therapy for hepatocellular carcinoma. *Nat Rev Gastroenterol Hepatol* 16(10): 617-630, 2019. PMID: 31371809. DOI: 10.1038/s41575-019-0179-x
- Faivre S, Rimassa L and Finn RS: Molecular therapies for HCC: Looking outside the box. *J Hepatol* 72(2): 342-352, 2020. PMID: 31954496. DOI: 10.1016/j.jhep.2019.09.010
- Marin JGG, Macias RIR, Monte MJ, Romero MR, Asensio M, Sanchez-Martin A, Cives-Losada C, Temprano AG, Espinosa-Escudero R, Reviejo M, Bohorquez LH and Briz O: Molecular bases of drug resistance in hepatocellular carcinoma. *Cancers* 12(6): 1663, 2020. PMID: 32585893. DOI: 10.3390/cancers12061663
- Rebouissou S and Nault JC: Advances in molecular classification and precision oncology in hepatocellular carcinoma. *J Hepatol* 72(2): 215-229, 2020. PMID: 31954487. DOI: 10.1016/j.jhep.2019.08.017
- Sia D, Villanueva A, Friedman SL and Llovet JM: Liver cancer cell of origin, molecular class, and effects on patient prognosis. *Gastroenterology* 152(4): 745-761, 2017. PMID: 28043904. DOI: 10.1053/j.gastro.2016.11.048
- Zucman-Rossi J, Vilanueva A, Nault JC and Llovet JM: Genetic landscape and biomarkers of hepatocellular carcinoma. *Gastroenterology* 149(5): 1226-1239, 2015. PMID: 26099527. DOI: 10.1053/j.gastro.2015.05.061
- Schulze K, Nault JC and Villanueva A: Genetic profiling of hepatocellular carcinoma using next-generation sequencing. *J Hepatol* 65(5): 1031-1042, 2016. PMID: 27262756. DOI: 10.1016/j.jhep.2016.05.035
- Totoki Y, Tatsuno K, Covington KR, Ueda H, Creighton CJ, Kato M, Tsuji S, Donehower LA, Slagle BL, Nakamura H, Yamamoto S, Shinbrot E, Hama N, Lehmkuhl M, Hosoda F, Arai Y, Walker K, Dahdouli M, Gotoh K, Nagae G, Gingras MC, Muzny DM, Ojima H, Shimada K, Midorikawa Y, Goss JA, Cotton R, Hayashi A, Shibahara J, Ishikawa S, Guiteau J, Tanaka M, Urushidate T, Ohashi S, Okada N, Doddapaneni H, Wang M, Zhu Y, Dinh H, Okusaka T, Kokudo N, Kosuge T, Takayama T, Fukayama M, Gibbs RA, Wheeler DA, Aburatani H and Shibata T: Trans-ancestry mutational landscape of hepatocellular carcinoma genomes. *Nat Genet* 46(12): 1267-1273, 2014. PMID: 25362482. DOI: 10.1038/ng.3126
- Schulze K, Imbeaud S, Letouzé E, Alexandrov LB, Calderaro J, Rebouissou S, Couchy G, Meiller C, Shinde J, Soysouvanh F, Calatayud AL, Pinyol R, Pelletier L, Balabaud C, Laurent A, Blanc JF, Mazzaferro V, Calvo F, Villanueva A, Nault JC, Bioulac-Sage P, Stratton MR, Llovet JM and Zucman-Rossi J: Exome sequencing of hepatocellular carcinomas identifies new mutational signatures and potential therapeutic targets. *Nat Genet* 47(5): 505-511, 2015. PMID: 25822088. DOI: 10.1038/ng.3252
- Lee IN, Chen CH, Sheu JC, Lee HS, Huang GT, Yu CY, Lu FJ and Chow LP: Identification of human hepatocellular carcinoma-

- related biomarkers by two-dimensional difference gel electrophoresis and mass spectrometry. *J Proteome Res* 4(6): 2062-2069, 2005. PMID: 16335951. DOI: 10.1021/pr0502018
- 13 Liang CR, Leow CK, Neo JC, Tan GS, Lo SL, Lim JW, Seow TK, Lai PB and Chung MC: Proteome analysis of human hepatocellular carcinoma tissues by two-dimensional difference gel electrophoresis and mass spectrometry. *Proteomics* 5(8): 2258-2271, 2005. PMID: 15852300. DOI: 10.1002/pmic.200401256
- 14 Sun W, Xing B, Sun Y, Du X, Lu M, Hao C, Lu Z, Mi W, Wu S, Wei H, Gao X, Zhu Y, Jiang Y, Qian X and He F: Proteome analysis of hepatocellular carcinoma by two-dimensional difference gel electrophoresis: novel protein markers in hepatocellular carcinoma tissues. *Mol Cell Proteomics* 6(10): 1798-1808, 2007. PMID: 17627933. DOI: 10.1074/mcp.M600449-MCP200
- 15 Strathmann J, Paal K, Itrich C, Krause E, Appel KE, Glauert HP, Buchmann A and Schwarz M: Proteome analysis of chemically induced mouse liver tumors with different genotype. *Proteomics* 7(18): 3318-3331, 2007. PMID: 17722141. DOI: 10.1002/pmic.200600983
- 16 Rousseau B, Ménard L, Haurie V, Taras D, Blanc JF, Moreau-Gaudry F, Metzler P, Hugues M, Boyault S, Lemièrre S, Canron X, Costet P, Cole M, Balabaud C, Bioulac-Sage P, Zucman-Rossi J and Rosenbaum J: Overexpression and role of the ATPase and putative DNA helicase RuvB-like 2 in human hepatocellular carcinoma. *Hepatology* 46(4): 1108-1118, 2007. PMID: 17657734. DOI: 10.1002/hep.21770
- 17 Teramoto R, Minagawa H, Honda M, Miyazaki K, Tabuse Y, Kamijo K, Ueda T and Kaneko S: Protein expression profile characteristic to hepatocellular carcinoma revealed by 2D-DIGE with supervised learning. *Biochim Biophys Acta* 1784(5): 764-772, 2008. PMID: 18359300. DOI: 10.1016/j.bbapap.2008.02.011
- 18 Minagawa H, Yamashita T, Honda M, Tabuse Y, Kamijo K, Tsugita A and Kaneko S: Comparative analysis of proteome and transcriptome in human hepatocellular carcinoma using 2D-DIGE and SAGE. *Protein J* 27(7-8): 409-419, 2008. PMID: 19048362. DOI: 10.1007/s10930-007-9123-y
- 19 Chafey P, Finzi L, Boisgard R, Caüzac M, Clary G, Broussard C, Pégrier JP, Guillonneau F, Mayeux P, Camoin L, Tavitian B, Colnot S and Perret C: Proteomic analysis of beta-catenin activation in mouse liver by DIGE analysis identifies glucose metabolism as a new target of the Wnt pathway. *Proteomics* 9(15): 3889-3900, 2009. PMID: 19639598. DOI: 10.1002/pmic.200800609
- 20 Corona G, De Lorenzo E, Elia C, Simula MP, Avellini C, Baccarani U, Lupo F, Tiribelli C, Colombatti A and Toffoli G: Differential proteomic analysis of hepatocellular carcinoma. *Int J Oncol* 36(1): 93-99, 2010. PMID: 19956837.
- 21 Liu Y, Li C, Xing Z, Yuan X, Wu Y, Xu M, Tu K, Li Q, Wu C, Zhao M and Zeng R: Proteomic mining in the dysplastic liver of WHV/c-MYC mice—insights and indicators for early hepatocarcinogenesis. *FEBS J* 277(19): 4039-4053, 2010. PMID: 20807235. DOI: 10.1111/j.1742-4658.2010.07795.x
- 22 Albrethsen J, Müller LM, Novikoff PM and Angeletti RH: Gel-based proteomics of liver cancer progression in rat. *Biochim Biophys Acta* 1814(10): 1367-1376, 2011. PMID: 21683810. DOI: 10.1016/j.bbapap.2011.05.018
- 23 Codarin E, Renzone G, Poz A, Avellini C, Baccarani U, Lupo F, di Maso V, Crocè SL, Tiribelli C, Arena S, Quadrifoglio F, Scaloni A and Tell G: Differential proteomic analysis of subfractionated human hepatocellular carcinoma tissues. *J Proteome Res* 8(5): 2273-2284, 2009. PMID: 19290626. DOI: 10.1021/pr8009275
- 24 Matos JM, Witzmann FA, Cummings OW and Schmidt CM: A pilot study of proteomic profiles of human hepatocellular carcinoma in the United States. *J Surg Res* 155(2): 237-243, 2009. PMID: 19535095. DOI: 10.1016/j.jss.2008.06.008
- 25 Ritorto MS and Borlak J: Combined serum and tissue proteomic study applied to a c-MYC transgenic mouse model of hepatocellular carcinoma identified novel disease regulated proteins suitable for diagnosis and therapeutic intervention strategies. *J Proteome Res* 10(7): 3012-3030, 2011. PMID: 21644509. DOI: 10.1021/pr101207t
- 26 Megger DA, Bracht T, Kohl M, Ahrens M, Naboulsi W, Weber F, Hoffmann AC, Stephan C, Kuhlmann K, Eisenacher M, Schlaak JF, Baba HA, Meyer HE and Sitek B: Proteomic differences between hepatocellular carcinoma and nontumorous liver tissue investigated by a combined gel-based and label-free quantitative proteomics study. *Mol Cell Proteomics* 12(7): 2006-2020, 2013. PMID: 23462207. DOI: 10.1074/mcp.M113.028027
- 27 Kimura K, Ojima H, Kubota D, Sakumoto M, Nakamura Y, Tomonaga T, Kosuge T and Kondo T: Proteomic identification of the macrophage-capping protein as a protein contributing to the malignant features of hepatocellular carcinoma. *J Proteomics* 78: 362-373, 2013. PMID: 23085225. DOI: 10.1016/j.jprot.2012.10.004
- 28 Tan GS, Lim KH, Tan HT, Khoo ML, Tan SH, Toh HC and Chung MCM: Novel proteomic biomarker panel for prediction of aggressive metastatic hepatocellular carcinoma relapse in surgically resectable patients. *J Proteome Res* 13(11): 4833-4846, 2014. PMID: 24946162. DOI: 10.1021/pr500229n
- 29 Reis H, Padden J, Ahrens M, Pütter C, Bertram S, Pott LL, Reis AC, Weber F, Juntermanns B, Hoffmann AC, Eisenacher M, Schlaak JF, Canbay A, Meyer HE, Sitek B and Baba HA: Differential proteomic and tissue expression analyses identify valuable diagnostic biomarkers of hepatocellular differentiation and hepatoid adenocarcinomas. *Pathology* 47(6): 543-550, 2015. PMID: 26308133. DOI: 10.1097/PAT.0000000000000298
- 30 Jin B, Gong Z, Yang N, Huang Z, Zeng S, Chen H, Hu S and Pan G: Downregulation of betaine homocysteine methyltransferase (BHMT) in hepatocellular carcinoma associates with poor prognosis. *Tumour Biol* 37(5): 5911-5917, 2016. PMID: 26592251. DOI: 10.1007/s13277-015-4443-6
- 31 Rong Z, Fan T, Li H, Li J, Wang K, Wang X, Dong J, Chen J, Wang F, Wang J and Wang A: Differential proteomic analysis of gender-dependent hepatic tumorigenesis in Hras12V transgenic mice. *Mol Cell Proteomics* 16(8): 1475-1490, 2017. PMID: 28512230. DOI: 10.1074/mcp.M116.065474
- 32 Zubaidah RM, Tan GS, Tan SBE, Lim SG, Lin Q and Chung MCM: 2-D DIGE profiling of hepatocellular carcinoma tissues identified isoforms of far upstream binding protein (FUBP) as novel candidates in liver carcinogenesis. *Proteomics* 8(23-24): 5086-5096, 2008. PMID: 19003864. DOI: 10.1002/pmic.200800322
- 33 Megger DA, Rosowski K, Ahrens M, Bracht T, Eisenacher M, Schlaak JF, Weber F, Hoffmann AC, Meyer HE, Baba HA and Sitek B: Tissue-based quantitative proteome analysis of human hepatocellular carcinoma using tandem mass tags. *Biomarkers* 22(2): 113-122, 2017. PMID: 27467182. DOI: 10.1080/1354750X.2016.1210678
- 34 Heindryckx F, Colle I and Van Vlierberghe H: Experimental mouse models for hepatocellular carcinoma research. *Int J Exp Pathol* 90(4): 367-386, 2009. PMID: 19659896. DOI: 10.1111/j.1365-2613.2009.00656.x

- 35 Bakiri L and Wagner EF: Mouse models for liver cancer. *Mol Oncol* 7(2): 206-223, 2013. PMID: 23428636. DOI: 10.1016/j.molonc.2013.01.005
- 36 Lambrecht C, Libbrecht L, Sagaert X, Pauwels P, Hoorne Y, Crowther J, Louis JV, Sents W, Sablina A and Janssens V: Loss of protein phosphatase 2A regulatory subunit B56 δ promotes spontaneous tumorigenesis *in vivo*. *Oncogene* 37(4): 544-552, 2018. PMID: 28967903. DOI: 10.1038/onc.2017.350
- 37 Louis JV, Martens E, Borghgraef P, Lambrecht C, Sents W, Longin S, Zwaenepoel K, Pijnenborg R, Landrieu I, Lippens G, Ledermann B, Götz J, Van Leuven F, Goris J and Janssens V: Mice lacking phosphatase PP2A subunit PR61/B δ (*Ppp2r5d*) develop spatially restricted tauopathy by deregulation of CDK5 and GSK3 β . *Proc Natl Acad Sci USA* 108(17): 6957-6962, 2011. PMID: 21482799. DOI: 10.1073/pnas.1018777108
- 38 Janssens V and Goris J: Protein phosphatase 2A: A highly regulated family of serine/threonine phosphatases implicated in cell growth and signalling. *Biochem J* 353: 417-439, 2001. PMID: 11171037. DOI: 10.1042/0264-6021:3530417
- 39 Haesen D, Sents W, Lemaire K, Hoorne Y and Janssens V: The basic biology of PP2A in hematologic cells and malignancies. *Front Oncol* 4: 347, 2014. PMID: 25566494. DOI: 10.3389/fonc.2014.00347
- 40 Reynhout S and Janssens V: Physiologic functions of PP2A: lessons from genetically modified mice. *Biochim Biophys Acta Mol Cell Res* 1866(1): 31-50, 2019. PMID: 30030003. DOI: 10.1016/j.bbamcr.2018.07.010
- 41 Meeusen B and Janssens V: Tumor suppressive protein phosphatases in human cancer: Emerging targets for therapeutic intervention and tumor stratification. *Int J Biochem Cell Biol* 96: 98-134, 2018. PMID: 29031806. DOI: 10.1016/j.biocel.2017.10.002
- 42 Sandgren EP, Quaife CJ, Pinkert CA, Palmiter RD and Brinster RL: Oncogene-induced liver neoplasia in transgenic mice. *Oncogene* 4(6): 715-724, 1989. PMID: 2543942.
- 43 Shachaf CM, Kopelman AM, Arvanitis C, Karlsson A, Beer S, Mandl S, Bachmann MH, Borowsky AD, Ruebner B, Cardiff RD, Yang Q, Bishop JM, Contag CH and Felsner DW: MYC inactivation uncovers pluripotent differentiation and tumour dormancy in hepatocellular cancer. *Nature* 431(7012): 1112-1117, 2004. PMID: 15475948. DOI: 10.1038/nature03043
- 44 Kaposi-Novak P, Libbrecht L, Woo HG, Lee YH, Sears NC, Coulouarn C, Conner EA, Factor VM, Roskams T and Thorgeirsson SS: Central role of c-MYC during malignant conversion in human hepatocarcinogenesis. *Cancer Res* 69(7): 2775-2782, 2009. PMID: 19276364. DOI: 10.1158/0008-5472.CAN-08-3357
- 45 Lee JS, Chu IS, Mikaelyan A, Calvisi DF, Heo J, Reddy JK and Thorgeirsson SS: Application of comparative functional genomics to identify best-fit mouse models to study human cancer. *Nat Genet* 36(12): 1306-1311, 2004. PMID: 15565109. DOI: 10.1038/ng1481
- 46 Martens E, Stevens I, Janssens V, Vermeesch J, Götz J, Goris J and Van Hoof C: Genomic organisation, chromosomal localisation tissue distribution and developmental regulation of the PR61/B δ regulatory subunits of protein phosphatase 2A in mice. *J Mol Biol* 336(4): 971-986, 2004. PMID: 15095873. DOI: 10.1016/j.jmb.2003.12.047
- 47 Nakashima O, Sugihara S, Eguchi A, Taguchi J, Watanabe J and Kojiro M: Pathomorphologic study of pale bodies in hepatocellular carcinoma. *Acta Pathol Jpn* 42: 414-418, 1992. PMID: 1323908. DOI: 10.1111/j.1440-1827.1992.tb03246.x
- 48 Moon WS, Yu HC, Chung MJ, Kang MJ and Lee DG: Pale bodies in hepatocellular carcinoma. *J Korean Med Sci* 15: 516-520, 2000. PMID: 11068987. DOI: 10.3346/jkms.2000.15.5.516
- 49 Liu Z, Ma Y, Yang J and Qin H: Upregulated and downregulated proteins in hepatocellular carcinoma: a systematic review of proteomic profiling studies. *OMICS* 15(1-2): 61-71, 2011. PMID: 20726783. DOI: 10.1089/omi.2010.0061
- 50 Thorgeirsson SS, Lee JS and Grisham JW: Functional genomics of hepatocellular carcinoma. *Hepatology* 43: S145-S150, 2006. PMID: 16447291. DOI: 10.1002/hep.21063
- 51 Hirata H, Sugimachi K, Komatsu H, Ueda M, Masuda T, Uchi R, Sakimura S, Nambara S, Saito T, Shinden Y, Iguchi T, Eguchi H, Ito S, Terashima K, Sakamoto K, Hirakawa M, Honda H and Mimori K: Decreased expression of fructose-1,6-bisphosphatase associates with glucose metabolism and tumor progression in hepatocellular carcinoma. *Cancer Res* 76(11): 3265-3276, 2016. PMID: 27197151. DOI: 10.1158/0008-5472.CAN-15-2601
- 52 Martínez-Chantar ML, Corrales FJ, Martínez-Cruz LA, García-Trevijano ER, Huang ZZ, Chen L, Kanel G, Avila MA, Mato JM and Lu SC: Spontaneous oxidative stress and liver tumors in mice lacking methionine adenosyltransferase 1A. *FASEB J* 16(10): 1292-1294, 2002. PMID: 12060674. DOI: 10.1096/fj.02-0078fje
- 53 Martínez-Chantar ML, Vázquez-Chantada M, Ariz U, Martínez N, Varela M, Luka Z, Capdevila A, Rodríguez J, Aransay AM, Matthiesen R, Yang H, Calvisi DF, Esteller M, Fraga M, Lu SC, Wagner C and Mato JM: Loss of the glycine N-methyltransferase gene leads to steatosis and hepatocellular carcinoma in mice. *Hepatology* 47(4): 1191-1199, 2008. PMID: 18318442. DOI: 10.1002/hep.22159
- 54 Yamaguchi M, Osuka S, Weitzmann MN, El-Rayes BF, Shoji M and Murata T: Prolonged survival in hepatocarcinoma patients with increased regucalcin gene expression: HepG2 cell proliferation is suppressed by overexpression of regucalcin *in vitro*. *Int J Oncol* 49(4): 1686-1694, 2016. PMID: 27633001. DOI: 10.3892/ijo.2016.3669
- 55 Yamaguchi M and Murata T: Exogenous regucalcin suppresses the growth of human liver cancer HepG2 cells *in vitro*. *Oncol Rep* 39(6): 2924-2930, 2018. PMID: 29620227. DOI: 10.3892/or.2018.6357
- 56 Hu L, Lau SH, Tzang CH, Wen JM, Wang W, Xie D, Huang M, Wang Y, Wu MC, Huang JF, Zeng WF, Sham JS, Yang M and Guan XY: Association of vimentin overexpression and hepatocellular carcinoma metastasis. *Oncogene* 23(1): 298-302, 2004. PMID: 14647434. DOI: 10.1038/sj.onc.1206483
- 57 Dai Z, Liu YK, Cui JF, Shen HL, Chen J, Sun RX, Zhang Y, Zhou XW, Yang PY and Tang ZY: Identification and analysis of altered alpha1,6-fucosylated glycoproteins associated with hepatocellular carcinoma metastasis. *Proteomics* 6(21): 5857-5867, 2006. PMID: 17068759. DOI: 10.1002/pmic.200500707
- 58 Shirahashi H, Sakaida I, Terai S, Hironaka K, Kusano N and Okita K: Ubiquitin is a possible new predictive marker for the reoccurrence of human hepatocellular carcinoma. *Liver* 22(5): 413-418, 2002. PMID: 12458564. DOI: 10.1034/j.1600-0676.2002.01541.x

Received August 28, 2020

Revised September 13, 2020

Accepted September 14, 2020